



Contents lists available at ScienceDirect

Colloids and Surfaces A: Physicochemical and Engineering Aspects

journal homepage: www.elsevier.com/locate/colsurfa

Foam-in-vein: Rheological characterisation of liquid sclerosing foams using a pipe viscometer

Alireza Meghdadi^{a,d}, Stephen A. Jones^b, Venisha A. Patel^b, Andrew L. Lewis^b, Timothy M. Millar^c, Dario Carugo^{d,*}

^a Faculty of Engineering and Physical Sciences, University of Southampton, Southampton, UK

^b Biocompatibles UK Ltd, Lakeview, Riverside Way, Watchmoor Park, Camberley, UK

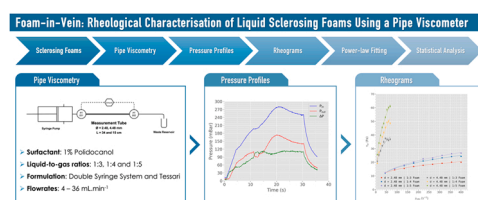
^c Faculty of Medicine, University of Southampton, Southampton, UK

^d Department of Pharmaceutics, School of Pharmacy, University College London, London, UK

HIGHLIGHTS

- The rheological behaviour of polidocanol-based sclerosing foams was evaluated.
- Foams of different liquid-to-gas ratios and manual production techniques were used.
- A novel therapeutically-relevant pipe viscometer was used to model foam behaviour.
- The effect of different clinically-relevant parameters on foam rheology was assessed.
- Lower injection rates and higher gas fractions resulted in more viscous foams.

GRAPHICAL ABSTRACT



ARTICLE INFO

Keywords:

Sclerosing foam
Aqueous foam
Sclerotherapy
Rheology
Pipe viscometry
Varicose vein treatment

ABSTRACT

Sclerotherapy is one of the most common and least-invasive treatment methods for varicose veins. While bench-top properties of sclerosing foams (e.g., bubble size distribution and foam half-life) have been studied previously, their flow behaviour and its relationship to therapeutic efficacy remain largely uncharacterised. To address this research gap, the present study reports on a novel approach for the rheological characterisation of sclerosing foams aimed at obtaining clinically-applicable data. A pipe viscometry apparatus was employed under conditions that mimic the end-point therapeutic application of foams. Polidocanol (1% v/v) foams of various liquid-to-gas volume ratios (1:3, 1:4 and 1:5) were formulated manually using the Tessari and DSS (double syringe system) methods across a clinically-relevant range of shear rates ($\approx 7 \text{ s}^{-1} - 400 \text{ s}^{-1}$), in polytetrafluoroethylene pipes of different diameters (2.48 mm and 4.48 mm). Additionally, end-effect and wall-slip correction methods were utilised to model the nominal rheology of sclerosing foams. The rheological data were fitted into a power-law model to obtain fluid flow index (n) and fluid consistency index (K) of sclerosing foams, followed by an in-depth statistical analysis of the power-law indices. The observed rheological behaviour of sclerosing foams is shown to be dependent on vessel diameter and liquid-to-gas ratio, while the type of manual formulation technique used appears to be statistically insignificant towards foam rheology. Sclerosing foams behaved as shear-thinning fluids with observed flow indices ranging $0.238 < n < 0.445$, while the observed consistency indices

* Corresponding author.

E-mail address: d.carugo@ucl.ac.uk (D. Carugo).

<https://doi.org/10.1016/j.colsurfa.2022.128916>

Received 18 January 2022; Received in revised form 29 March 2022; Accepted 31 March 2022

Available online 3 April 2022

0927-7757/© 2022 The Author(s). Published by Elsevier B.V. This is an open access article under the CC BY license (<http://creativecommons.org/licenses/by/4.0/>).

ranged $2.977 < K < 12.49$. The nominal (end-effect corrected) rheology of foams was shown to follow similar trends concerning liquid-to-gas ratio and formulation technique, independent of the tube diameter. The power-law characterisation of sclerosing foam rheology provided evidence of a quasi-static drainage effect that affected foam viscosity during slower injections. Wall-slip correction failed to provide physically meaningful results and statistical analysis suggested that the type of manual formulation technique used has no impact on the outcome of sclerotherapy on larger varicosities. Overall, results suggest a direct correlation between foam dryness and viscosity. Based on the developed rheological model, this work also demonstrates that low injection flowrates could yield higher therapeutic efficacy in dilated varicose veins.

1. Introduction

Sclerosing foam formulations are routinely administered for varicose vein therapy. Most commonly, sclerosing foams are produced as needed by mixing a surfactant solution with room air at different liquid-to-gas (L:G) volume ratios using syringes. Following production, they are administered intravenously using a needle or a catheter into diseased veins [1]. Various methods can be used to evaluate foam attributes, such as those providing a quantification of foam half-life and bubble size distribution [2]. While the dependence of these attributes on different factors like syringe and needle size, surfactant concentration, gas type and liquid-to-gas ratio have been studied extensively [1,3–7], the flow properties of sclerosing foams remain uncharacterised concerning their thixotropic (i.e., time-dependent) rheological nature.

Sclerosing foams are dynamic colloidal systems that continuously age over time. Gravity and capillary forces govern the ageing of foam; gravity pulls the liquid content of foam downwards while capillary forces drive it upwards. With gravity as the dominant force, ageing results in drainage of the surfactant solution from within the foam structure [8]. It has been demonstrated that shearing aqueous foams through a pipe, coupled with the ageing phenomenon, leads to the formation of a liquid film at the inner walls of a conduit that causes slippage [9]. The observed slipping shear rate will differ from the nominal slip-independent shear rate as a result of this phenomenon. Some studies paste sandpaper on rheometer walls to prevent slippage [7,10,11] while others utilise mathematical tools – such as the Oldroyd-Jastrzebski method – for correction of wall slip [9,12–14]. Recently, Wong et al. carried out conventional cone-plate rheometry on a variety of sclerosing foams while eliminating the wall-slip phenomenon using sandpaper. Their work is one of the very few studies that report on the rheological properties of sclerosing foams. However, thixotropic effects are not evaluated in this previous study and the utilised rheological model is not specifically defined [7]. Critello et al. evaluated the rheology of polidocanol-based sclerosing foams using a cone-plate rheometer although the effect of wall-slip is not eliminated (neither sandpaper nor mathematical techniques were employed), making comparison of results between the works of Wong et al. and Critello et al. virtually impossible [15].

Correcting the effect of wall-slip would yield nominal rheology of sclerosing foams and thus a valuable contribution to the characterisation of a foam's rheology is achievable. However, it may also eliminate the observed mechanical behaviour of foams that is exerted on the vascular endothelium during sclerotherapy. Nevertheless, it is still useful to correct for wall-slip to enable comparison with previous studies that utilise correction methods (mathematical or experimental). It has also been shown previously by several studies [9,13,16] that the history of shearing plays an important role in aqueous foam rheology. Therefore, to develop an application-specific rheological model a rheometry apparatus must mimic the end-point application of sclerosing foams. A suitable method of rheometry with the potential of wall-slip correction is pipe viscometry, which is also geometrically more therapeutically-relevant in nature when applied to sclerosing foams.

In contrast to conventional rheometry, pipe viscometry can not only mimic vascular flow with respect to the fluid velocity profile and the resulting wall shear stress, but it can also mimic the flow behaviour of

foam that would occur during a typical sclerotherapy treatment. Previously, pipe viscometry has been employed to characterise aqueous foams used in the petroleum industry [9], fire extinguishers [13] and other types of aqueous foams [12,16,17]. In principle, a typical pipe viscometer utilises a tube of known length (L) and inner diameter (d) and measures the pressure difference (ΔP) along the tube while the fluid of interest is sheared inside the tube under a constant flowrate. Flowrate (Q) is converted into observed shear rate ($\dot{\gamma}_{obs}$) given a laminar flow regime, as shown in Eq. 1, while the pressure differential values (ΔP) can be used to calculate wall shear stress (τ_w), as shown in Eq. 2 [9,18].

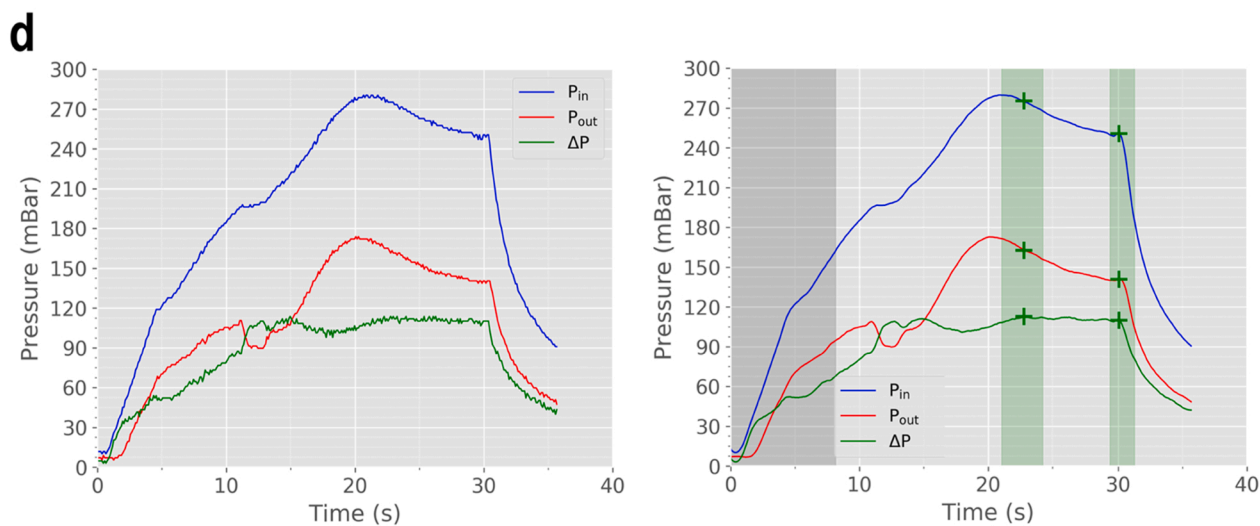
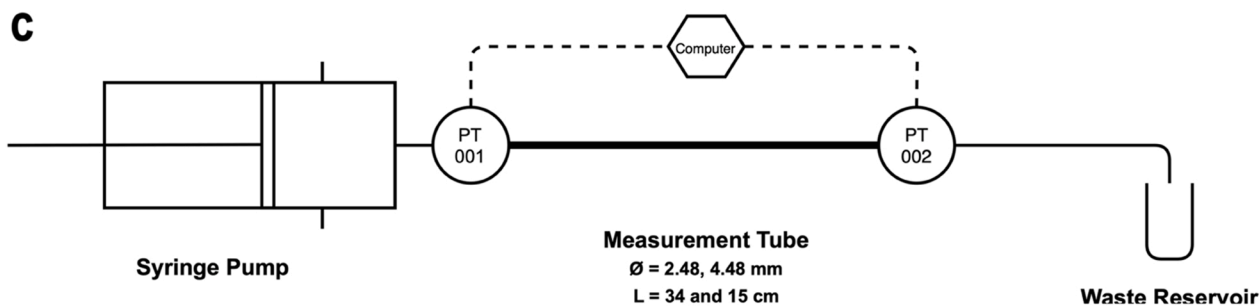
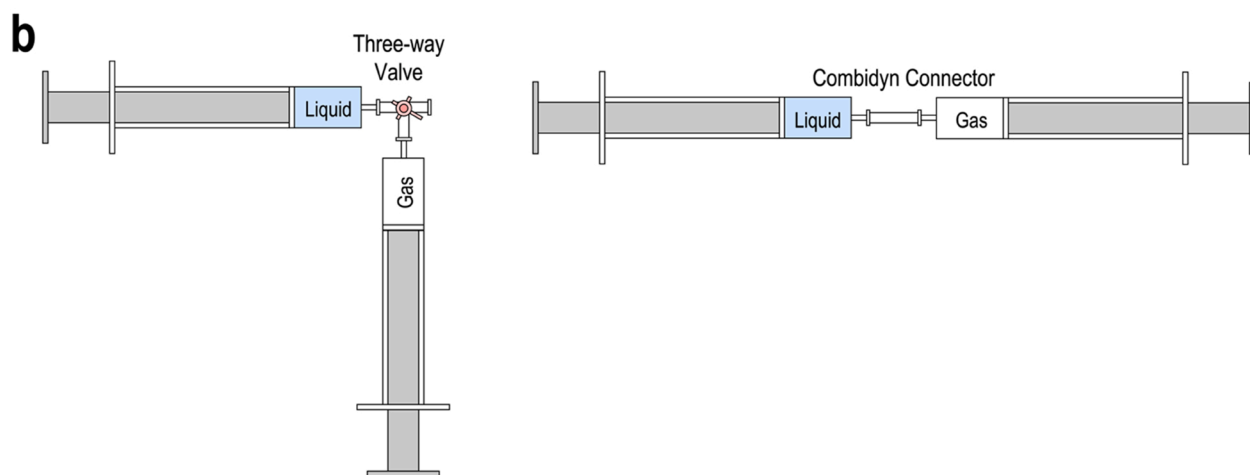
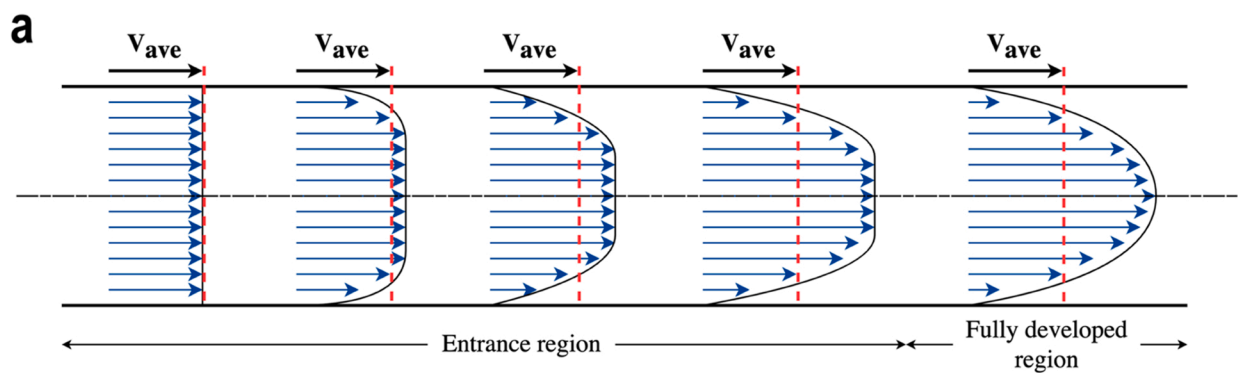
$$\dot{\gamma}_{observed} = \frac{32Q}{\pi d^3} \quad (1)$$

$$\tau_w = \frac{d\Delta P}{4L} \quad (2)$$

Plotting the wall shear stress data against the observed shear rate yields a rheogram that is then used to model the rheological behaviour of a given fluid. In addition, pipe viscometry using pipes of different diameters allows for the correction of wall-slip, the presence of which has been demonstrated in numerous studies [9,12,13,16]. In contrast to the observed rheological behaviour of a fluid, wall-slip correction would yield the nominal (true) rheological model. On entrance of a fluid into a tube, the fluid must travel a certain entrance length for its velocity profile to fully develop into Poiseuille flow (see Fig. 1a). Additionally, fittings used in the measurement apparatus would disturb the flow of fluid upon entrance and exit into and out of the pipe viscometer. A pressure drop is imposed on the system because of this so-called end-effect that needs to be accounted for. Most commonly, a long tube segment would allow for flow to fully develop before taking pressure measurements [19], as described in previous pipe viscometry studies of aqueous foams [9,12,13]. In contrast, the production of sclerosing foams is not a continuous process and is performed using low-capacity syringes. Thus, it is not possible to produce and inject sufficient sclerosing foam to prime the entire tube and allow the pressure profiles to plateau while providing the required tube length for the hydrodynamic flow to fully develop. Alternative methods of end-effect correction are therefore required. In this study, the Bagley method has been applied to the observed rheological data [19,20].

While end-effects affect the nominal pressure drop across the tube, wall-slip affects the nominal shear rate. Thus, wall-slip correction was conducted on end-effect corrected data to obtain a nominal rheological model of sclerosing foams using the Oldroyd-Jastrzebski slip correction method. This method has proven effective in calculating slip velocity in numerous previous studies [9,12–14] and was hence applied to the data obtained in this work by constructing graphs plotting $\dot{\gamma}_{obs}$ against $1/d^2$, at constant τ_w .

This work describes a therapeutically-relevant pipe viscometry apparatus utilised for the first time to provide an analytical characterisation of physician compounded foam (PCF) rheology in a clinically-relevant context. A wide range of conditions was tested including different foam production techniques (DSS and Tessari) and liquid-to-gas volumetric ratios (L:G ratios of 1:3, 1:4 and 1:5). PCFs were injected into polytetrafluoroethylene tubes of different inner diameters (2.48 mm ID and 4.48 mm ID) under a range of flowrates (4.00 – 36.0 mL.min⁻¹), and experiments were designed to allow for wall-slip



(caption on next page)

Fig. 1. a) The velocity profile of a fluid injected into a tube in the entrance region. Upon injection, the velocity profile begins to hydrodynamically develop into a Poiseuille flow. As a result of this entrance region, a pressure drop is experienced by the system that needs to be accounted for during rheological characterisation. b) Syringe arrangements used to create PCFs. The surfactant solution (1% POL) is pushed out of the 5 mL syringe into and out of the 10 mL syringe (holding room air) ten times. The volumetric ratio of gas and surfactant defines a PCF's liquid-to-gas ratio. Left: The Tessari method. A three-way valve with a 30° offset is used to connect syringes that creates Tessari foams. Right: The Double Syringe System (DSS). Syringes are connected using a Combidyn adapter when producing DSS foams. c) The pipe viscometry apparatus. PCFs are injected into the measurement tube using a syringe pump with a 10 mL silicone-free Norm-Ject™ syringe. A computer interface is connected to the two pressure transducers (PT 001 and PT 002) that measure and record static pressure. d) Representative pressure profiles obtained from the pipe viscometer. Left: Raw data before processing. Right: Processed data, showing the loci of first and final points of the ΔP plateau region (dark grey region: the time it takes for the tube to be fully primed with foam).

correction. Results suggest a direct correlation between foam dryness and viscosity, and - based on the developed rheological model - it also demonstrates that low injection flowrates could yield higher therapeutic efficacy in dilated varicose veins. Future studies will focus on correlating the obtained rheological data with readouts of therapeutic performance to inform the optimisation of current foam formulation and administration techniques.

2. Materials and methods

A pipe viscometry apparatus was designed and utilised to measure pressure differential along tubes of defined lengths and diameters. The recorded data were processed and converted to rheograms using Python. The resulting rheological data were fitted into a power-law model, while statistical tests were carried out to accurately characterise and evaluate the interactions between independent variables (tube ID, foam production method, and L:G ratio) and rheological properties of foams. The following provides details of the experimental procedures of pipe viscometry.

2.1. PCF formulations

In this study, a 1% v/v polidocanol (POL) solution in phosphate buffered saline (Croda, Goole, UK) was used as a sclerosing agent as this is a commonly administered POL formulation by clinicians and it achieves almost identical outcomes compared to more concentrated POL formulations [21,22]. PCFs were created using silicon-free Norm-Ject™ syringes (BD Biosciences, USA). Two different PCF production methods were utilised to produce 10 mL of foam at a time. In the double syringe system (DSS) method [23], the desired volume of liquid sclerosant is placed in a 5 mL syringe and is pushed in and out of a 10 mL syringe holding the required volume of room air, 10 times through a Combidyn connector (B. Braun Melsungen, Germany). In the Tessari (TSS) method [24], the Combidyn connector is replaced with a three-way valve (Cole-Parmer, UK) with an offset of 30° [8] (Fig. 1b). The volumes of liquid sclerosant and room air were 2.5 mL and 7.5 mL (L:G ratio = 1:3), 2.0 mL and 8.0 mL (L:G ratio = 1:4), and 8.35 mL and 1.65 mL (L:G ratio = 1:5).

2.2. Pipe Viscometry

Table 1 summarises the experimental parameters of this work. To avoid injecting the continuously drained liquid into the pipe viscometer, it was decided to only inject 8 mL of the formulated foam. Additionally, the syringe pump was slightly elevated at the syringe side, keeping the drained liquid away from the syringe outlet and thus holding it inside the syringe throughout injection. This also kept any exogenous air

pockets that would not normally be injected during clinical administration, away from the syringe outlet.

The pipe viscometer apparatus utilised a segment of translucent polytetrafluoroethylene (PTFE) tubing (Cole-Parmer, UK) with inner diameters (IDs) of 2.48 and 4.48 mm. The PTFE tubes were flanked by two MPS2 pressure transducers (Elveflow, Paris) with measurement limits of 1000 ± 3 mbar. PCFs were injected into the pipe viscometer using a PHD 2000 programmable syringe pump (Harvard Apparatus, UK). After formulating the foam, the syringe containing foam was placed on the pump and locked into a Luer-to-Barbed connector attached to a flexible silicon tube of length 4 cm and ID of 2.06 mm connected to the inlet pressure transducer. The outlet pressure transducer led to a waste beaker via silicone tubing. Injected PCFs were collected and discarded at the end of each experiment. Fig. 1c illustrates an instrumentation diagram of the pipe viscometer apparatus (see [Supplementary Material](#) Section ¶S.1.1 for a photographic image of the pipe viscometer).

Given the use of different tube IDs, different tube lengths were utilised to fill the tubes with foam and allow the pressure curves to plateau. Tube lengths of 34 cm and 15 cm were used for IDs of 2.48 and 4.48 mm, respectively. The pressure transducer was fitted directly onto the 2.48 mm ID tube. However, due to the increased size of the 4.48 mm ID tube, conical connectors were created using polydimethylsiloxane (PDMS) produced by mixing a pre-polymer with a curing agent (Sylgard® 184, Dow Corning Corporation, USA). This had the added benefit of reducing turbulence and shearing, which could affect the microstructure of the foam. This would be caused by the significant change in conduit diameter from the small ID of the transducer to the relatively large ID of the 4.48 mm tube, which could systematically affect the pressure profiles. Details of the production methods for these connectors are provided in the [Supplementary Material](#) (Section ¶S.1.2).

2.3. Data analysis

Pressure profiles showed a consistent behaviour among all experiments. Typically, inlet and outlet pressure signals rise as foam enters the pipe viscometer. When the pipe is fully primed with foam, pressure difference plateaus, and subsequently falls when injection stops (Fig. 1d). Signals were processed with a Python script that detected and trimmed the stable plateau region of pressure differentials. Additional details of recording and processing of pressure signals are outlined in the [Supplementary Material](#) (Sections ¶S.1.3 and ¶S.1.4).

2.3.1. Rheological calculations

The plateau region was averaged for each repeat (ΔP_{ave}) and the corresponding standard deviation was calculated. ΔP_{ave} values of three repeats were averaged to result in a mean pressure change (ΔP). To obtain rheograms, flowrate (Q) and pressure change (ΔP) values were

Table 1

Summary of experimental parameters of pipe viscometry experiments. ID: tube inner diameter; PCF: physician-compounded foam; DSS: double syringe system; TSS: Tessari.

	Volume of Foam	PCF Formulations	Flowrates	Tube ID	Tube Length	Shear Rates	Repeats
Pipe Viscometry	8 mL	DSS 1:3, 1:4, 1:5 TSS 1:3, 1:4, 1:5	4.00 – 36.0 mL.min ⁻¹ (4.00 mL.min ⁻¹ intervals)	2.48 mm 4.48 mm	34 cm 15 cm	44.5 – 401 s ⁻¹ 7.55 – 68.8 s ⁻¹	3

transformed – via Eq. (1) and Eq. (2) – to observed shear rate ($\dot{\gamma}_{obs}$) and wall shear stress (τ_w), where d is tube inner diameter and L is tube length. During plateau detection, injections at lower flowrates exhibited a decline of ΔP after it plateaued that may be attributed to the drainage phenomenon occurring quasi-statically during injection. To characterise this observation, $\overline{\Delta P}_{min}$ and $\overline{\Delta P}_{max}$ (the maximum and minimum $\overline{\Delta P}$ values of the trimmed plateau region) were used to calculate τ_{wmin} and τ_{wmax} , which were used to generate a min-max region on the rheograms (see Fig. S5 and Fig. S6) [13,16]. Further information on data processing methods utilised to obtain rheograms containing min-max regions is available in the [Supplementary Material](#) (Section ¶S.1.5).

The power-law equation (Eq. 3) was used to fit the rheological data. A power-law fluid is characterised by a fluid consistency index (K) and a fluid flow index (n). Eq. (3) was subsequently linearised, by applying a natural logarithmic function. The rheological data was then fitted into the linearised power-law equation (Eq. 4) using Prism 9 (Graphpad Software Inc., USA) to obtain the power-law indices.

$$\tau_w = K \dot{\gamma}_{obs}^n \quad (3)$$

$$\ln(\tau_w) = n \ln \dot{\gamma}_{obs} + \ln K \quad (4)$$

Apparent viscosity (μ_{app}) was then calculated using Eq. (5).

$$\mu_{app} = K \dot{\gamma}_{obs}^{n-1} \quad (5)$$

To demonstrate the flow regime of the sclerosing foams, the computed apparent viscosity profiles were used to calculate Reynolds numbers (assuming constant foam density) for each experiment, using Eq. (6).

$$Re = \frac{\rho_{foam} u d}{\mu_{app}} \quad (6)$$

Where ρ_{foam} is foam density, u is linear fluid velocity, and d is pipe diameter. ρ_{foam} was calculated as:

$$\rho_{foam} = (\phi_l * \rho_l) + (\phi_g * \rho_g) \quad (7)$$

Where ϕ_l and ϕ_g are liquid (1% POL) and air volume fractions, and ρ_l and ρ_g are liquid and air densities. ρ_{foam} can be estimated as $\rho_{foam} \approx (\phi_l * \rho_l)$ assuming negligible air density relative to the 1% POL density. The density of 1% POL solution (ρ_l) was considered to be 970 kg.m [39].

2.3.2. End-effect correction

To correct for end-effects, second-order polynomial fits (via the NumPy library in Python – np.polyfit) were used on the $\overline{\Delta P} - \dot{\gamma}_{obs}$ data to calculate smoothed $\overline{\Delta P}$ values at each employed flowrate. By plotting the resulting $\overline{\Delta P}$ values against L/d and fitting flowrate isometric lines through plotted $\overline{\Delta P}$ values, Bagley plots were produced. The y-intercept of the Bagley plots is regarded as pressure loss due to end-effects and was subtracted from original $\overline{\Delta P}$ values, to yield $\overline{\Delta P}$ data corrected for end-effects (ΔP_c) [19]. Rheograms were constructed for both corrected and uncorrected pressure data for comparison.

2.3.3. Wall-slip correction

To correct for wall-slip, a set of constant τ_w values were defined and used to calculate corresponding $\dot{\gamma}_{obs}$ values using a polynomial fit [25]. The Oldroyd-Jastrzebski slip correction graphs were constructed by plotting $\dot{\gamma}_{obs}$ against $1/d^2$, at constant τ_w . The slope of this plot would be equal to $8\tau_w\beta$. The slip coefficient (β) could then be plotted against τ_w and the relationship $\beta = a\tau_w + b$ could be obtained via linear regression, and used to calculate slip rate at any given wall shear stress value. Finally, nominal (true) shear rate can be calculated as follows:

$$\dot{\gamma}_{true} = \dot{\gamma}_{obs} - \frac{8\tau_w(a\tau_w + b)}{d^2} \quad (8)$$

2.3.4. Statistical analysis

Prism 9 (Graphpad Software Inc., USA) was used to conduct the required statistical tests. The effect of tube diameter on foam behaviour was evaluated by conducting unpaired nonparametric Mann – Whitney tests on power-law indices. To evaluate the interaction between foam formulation and foam rheology, two-way ANOVA (Analysis of Variance) tests were conducted on power-law indices and their respective errors. ANOVA tests were conducted under constant tube ID to avoid cross comparison between data sets uncorrected for wall-slip, due to the complications during wall-slip correction. Moreover, details of error propagation methods are given in the [Supplementary Material](#) (Section ¶S.1.6).

3. Results

3.1. End-effect correction

Pressure differentials (ΔP) associated with all experiments are plotted in Fig. 2. Using the data in Fig. 2, Bagley plots were created following the steps described in Section 2.3.2 and are illustrated in Fig. 3. The y-intercepts of this plot represent pressure loss due to end-effects.

3.2. Wall-slip correction

Following pressure correction, an attempt was made to correct for wall-slip, as outlined in Section ¶2.3.3. The Oldroyd-Jastrzebski plots are illustrated in Fig. 4. Oldroyd-Jastrzebski plots must yield non-negative y-intercept values. The experimental work in this study, however, resulted in negative y-intercepts, which are physically meaningless. The presence of negative y-intercepts prohibited further steps of wall-slip correction. The ramifications of this observation are discussed in more detail in Section ¶4.1.

3.3. Rheograms

Following end-effect correction, the rheological data are categorised into two groups henceforth. Data before end-effect correction will be referred to as “observed” data, and end-effect corrected data will be referred to as “nominal” data. Nominal rheograms, alongside corresponding power-law and statistical results, are included in [Supplementary Material](#) (Section ¶S.2.4) while the observed rheological data are outlined in Fig. 5. In the small tube (2.48 mm ID) observed wall shear stress (τ_w) ranges $\sim 11.96 - 26.67$ Pa while in the larger tube (4.48 mm ID) it ranges $\sim 19.17 - 60.96$ Pa (see Fig. 5c). Moreover, Fig. 5a and Fig. 5b show that rheograms of DSS foam cover a broader range of τ_w compared to those of TSS foams in both tubes, indicating that the rheology of sclerosing foams produced via the DSS technique is more sensitive to variations in L:G ratio. It is also evident that rheograms are grouped according to tube ID. This may be attributed to the presence of wall-slip. Theoretically, calculating slip rate and obtaining true shear rate is sufficient in bringing together data obtained using different tubes.

In addition to the rheograms, the Reynolds numbers corresponding to each experiment were calculated and are illustrated in the [Supplementary Material](#) (Fig. S7). These calculations show that the flow of sclerosing foams in this work is laminar.

3.4. Viscosity profiles

Observed rheograms were converted to apparent viscosity curves using Eq. (5) and are illustrated in Fig. 6. Apparent viscosities were found to be in the range $\sim 0.051 - 0.281$ Pa.s (measured in the 2.48 mm ID tube) and $\sim 0.568 - 3.40$ Pa.s (measured in the 4.48 mm ID tube). Viscosity profiles in Fig. 6 show that drier foams exhibit greater viscosities. This effect, however, is independent of tube ID, although apparent viscosity profiles of foams of different liquid-to-gas ratios are

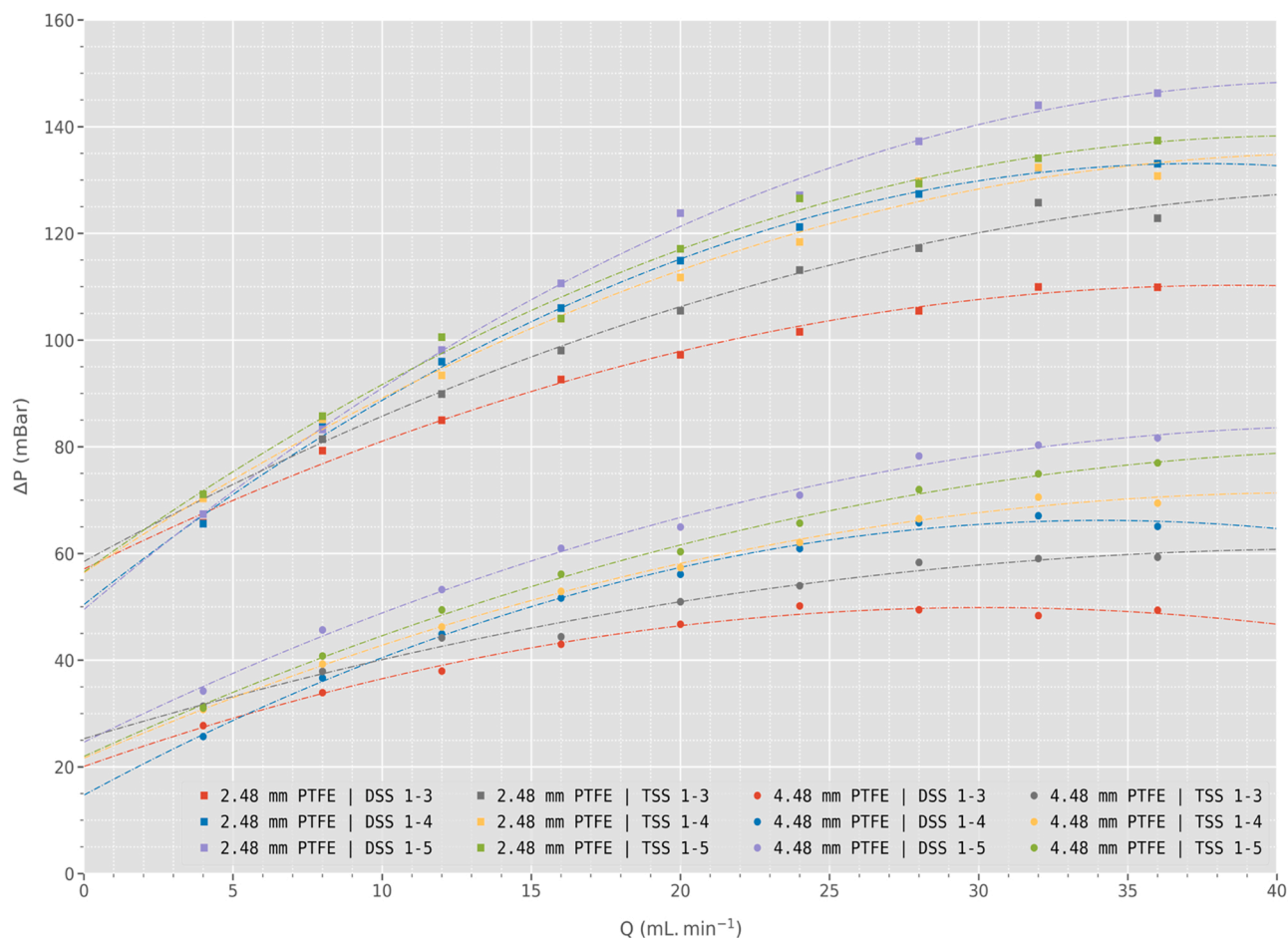


Fig. 2. ΔP values corresponding to all experiments plotted against injection flowrate (Q). Dotted lines represent second order polynomial fits that were used to obtain smoothed ΔP values at given flowrates. Squares represent data obtained using the 2.48 mm ID tube, while circles represent data obtained using the 4.48 mm ID tube. The pressure differentials obtained in the larger tube are generally smaller, although the shorter length of the 4.48 mm ID tube could also contribute to this difference.

more spread out in the larger (4.48 mm ID) tube.

3.5. Power-law indices

Linear regression was carried out on the observed data fitted into Eq. (4). Fig. 7 summarises these results. The slope (n) and y-intercept ($\ln K$) of each line were calculated alongside their associated standard error of the mean (SEM). The power-law indices of observed data were thus derived and are reported in Table 2.

3.6. Statistical analysis

This section includes various statistical test results obtained in this study.

3.6.1. Effect of conduit diameter

A comparison of power-law indices obtained using different tube sizes are summarised in Fig. 7c and Fig. 7d. Results of Mann – Whitney tests on the indices indicate a statistically significant difference between power-law indices of observed data. However, after end-effect correction, K values obtained through both tube types show no statistical difference while statistically significant differences were found among n values (see Fig. S10c and Fig. S10d).

3.6.2. Effect of foam formulation

The effect of liquid-to-gas ratio and formulation technique on the

rheological behaviour of sclerosing foams was evaluated by conducting two-way ANOVA on power-law indices obtained from regression analysis of observed data (ANOVA results of nominal data are included in Supplementary Section S.2.4). The significance of each factor (L:G ratio and foam production technique) was evaluated and a p-value was calculated in Prism. Table 3 summarises the extent of interaction associated with each factor. Different types of manual formulation technique make no significant difference to power-law indices of observed data in the larger tube. After end-effect correction (see Table S2), formulation technique remains statistically insignificant in the larger tube. With end-effect correction, the L:G ratio in the larger tube remains statistically significant although at a lower level of significance ($p_n = 0.03$ and $p_K = 0.05$ compared to both p_n and $p_K < 0.001$ without end-effect correction, see Table S2). Upon modelling the interaction of each factor on the power-law indices of observed data, detailed results of ANOVA are illustrated in Fig. 8 (summarising the effect of L:G ratio on power-law indices) and Fig. 9 (summarising the effect of formulation technique on power-law indices).

It should be noted that the results of two-way ANOVA on the power-law indices do not reflect on the statistical significance of viscosity profile differences directly. While in some cases both n and K values show significant differences, in other cases only one index is statistically different while the other is not. In such cases, viscosity profiles may not necessarily be statistically different. Table 4 and Table 5 summarise how two-way ANOVA results of the power-law indices reflect on apparent viscosity profiles.

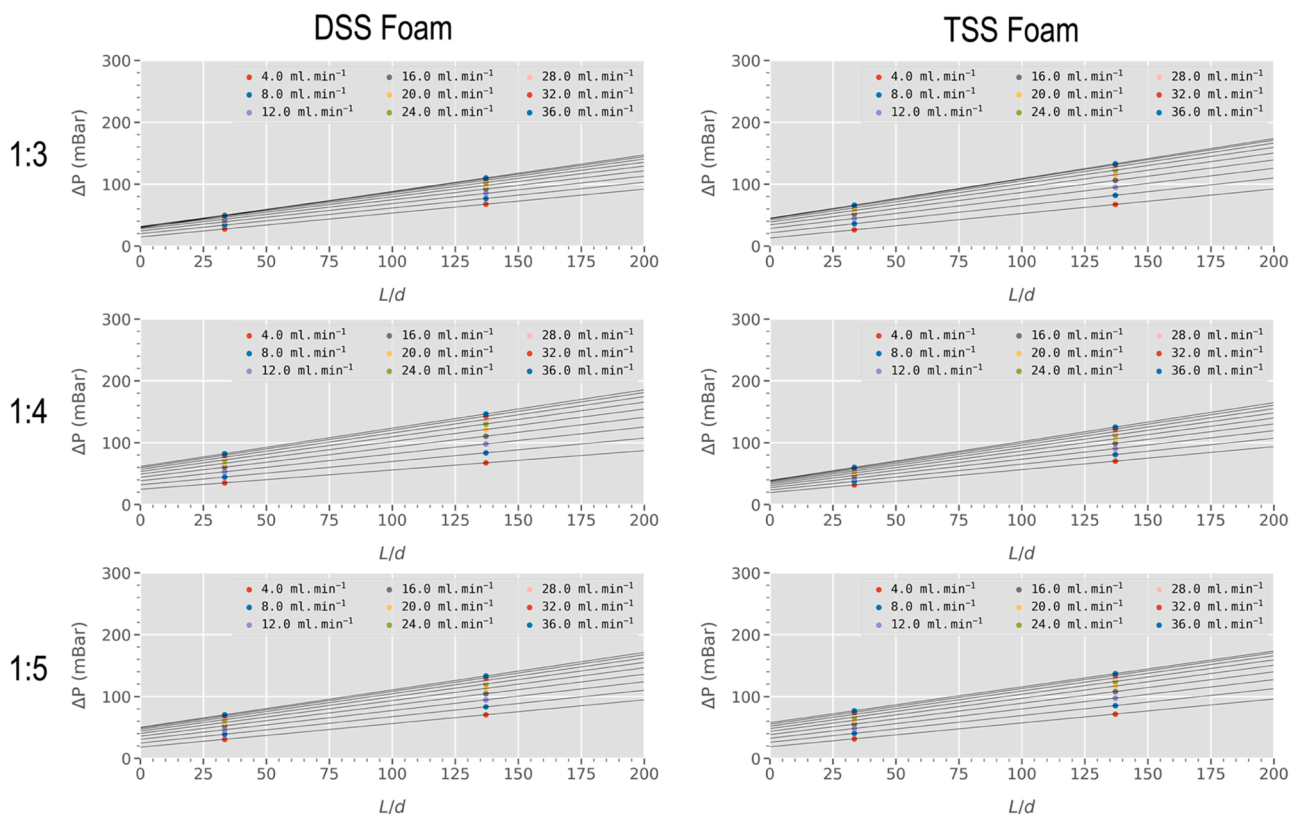


Fig. 3. The Bagley plots corresponding to foams of different formulations and L:G ratios (L:G ratio values are reported on the left). Linear regression was applied to obtain y-intercepts, which represent pressure loss due to end-effects and were used to correct ΔP values.

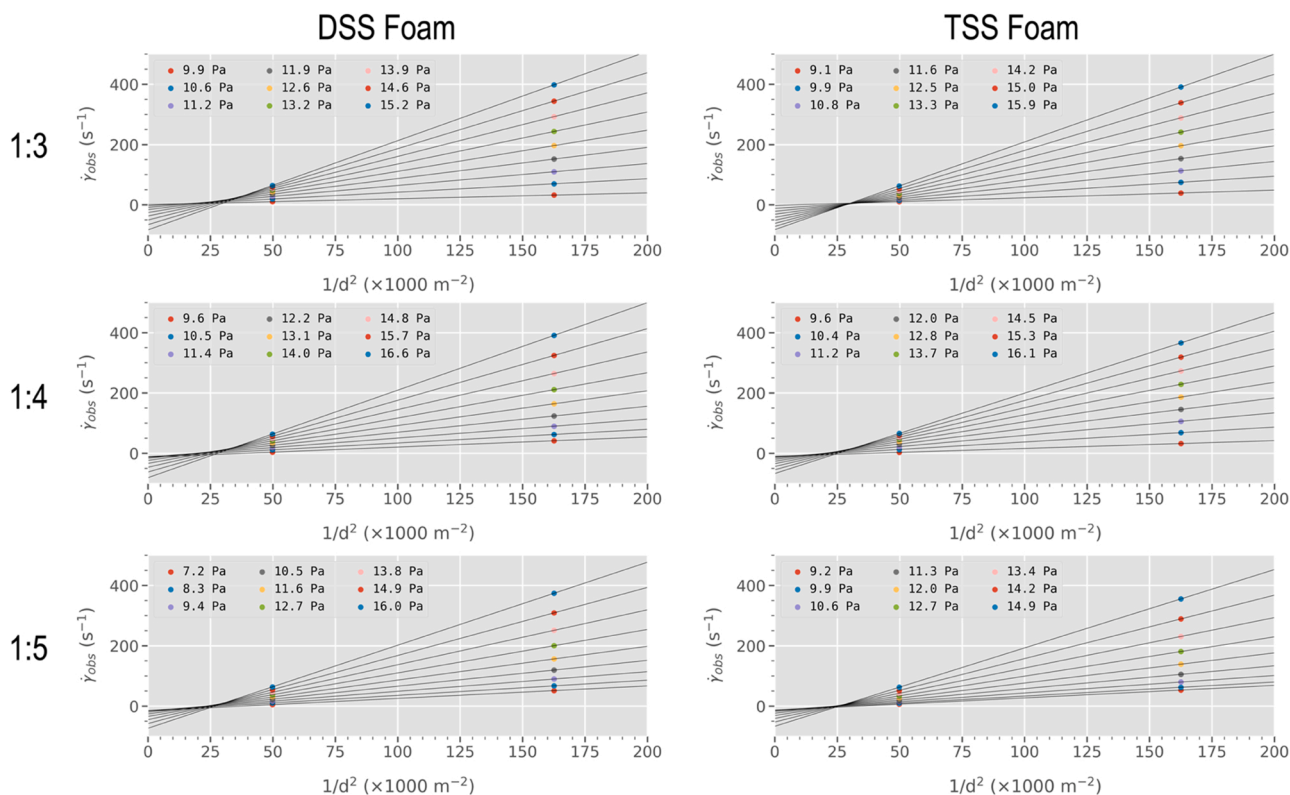


Fig. 4. Oldroyd-Jastrzebski wall-slip correction graphs construction, by plotting shear rate values against $1/d^2$ for given wall shear stress values. Solid lines are associated with constant wall shear stress values. Negative y-intercepts are physically meaningless and prohibited further progress in wall-slip correction.

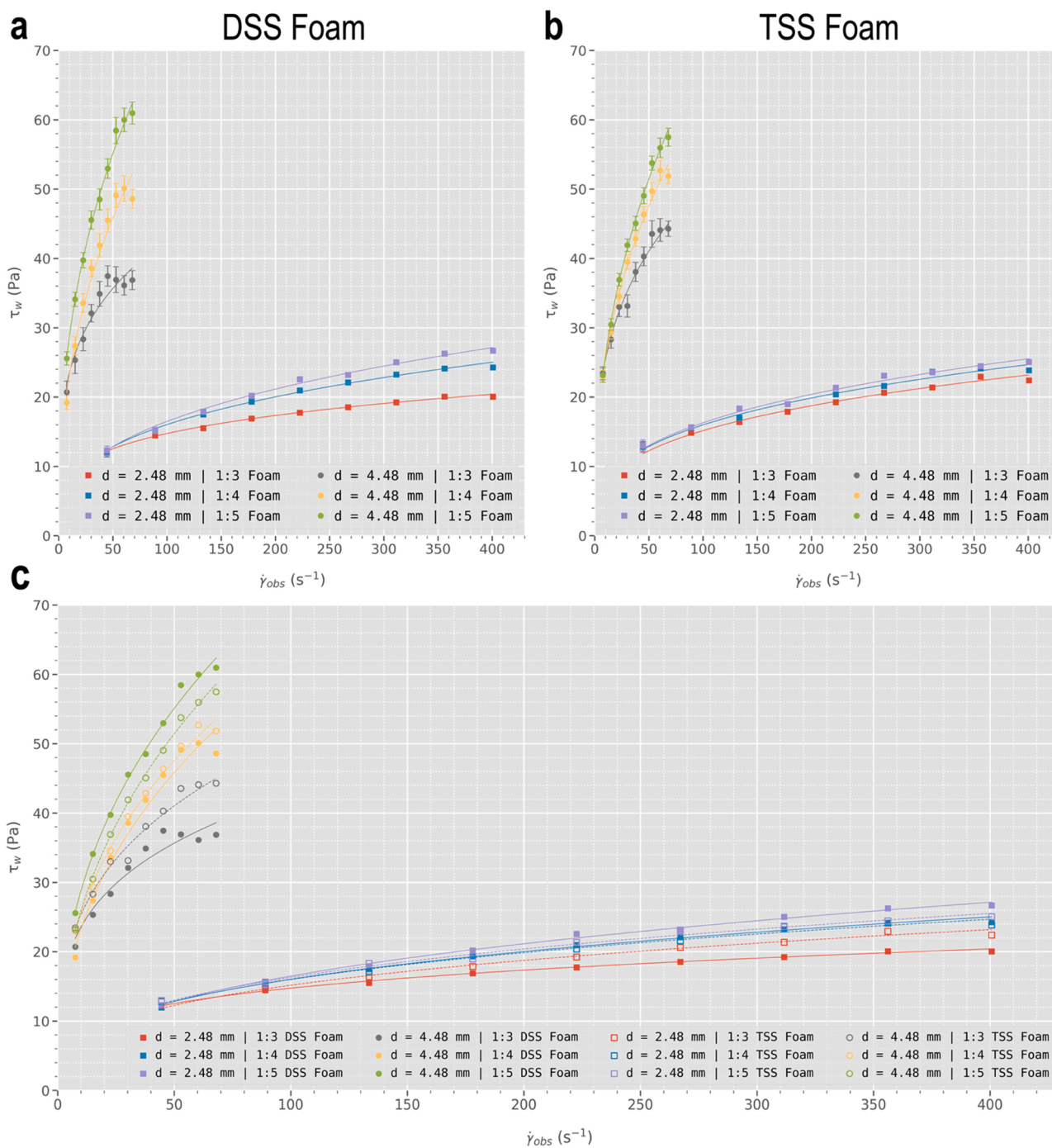


Fig. 5. Observed rheograms. Rheograms of (a) DSS and (b) TSS foams with non-linear power-law fits. Segregation of data into two groups is attributed to the wall-slip phenomenon. c) Superimposed rheograms of all 12 experiments (filled marks = DSS foam, empty marks = TSS foam). The data illustrated in this figure are not corrected for end-effects.

4. Discussion

Sclerotherapy is an effective treatment for varicose veins. However, pathological endothelial cells that survive treatment can lead to recurrence of varicosities [26], which is due to sub-optimal contact between the venous walls and the sclerosing agent. A more pervasive understanding of the flow behaviour of sclerosing foams could thus inform the design of more effective formulation and administration techniques. Previous research utilises conventional rheometric apparatuses [7,8] that cannot mimic therapeutically relevant conditions, such as venous geometry and foam injection rate. Consequently, clinical applicability of

rheological data modelled via these methods is hindered due to the shear-history sensitivity of sclerosing foams. In order to address these limitations, this work reports on the first application of pipe viscometry as a means to characterise the rheology of sclerosing foams under conditions that more closely mimic their end-point administration.

4.1. Flow rheology of sclerosing foams: considerations on wall-slip correction

The occurrence of wall-slip would result in higher observed shear rates, in turn yielding greater foam viscosity values given the positively

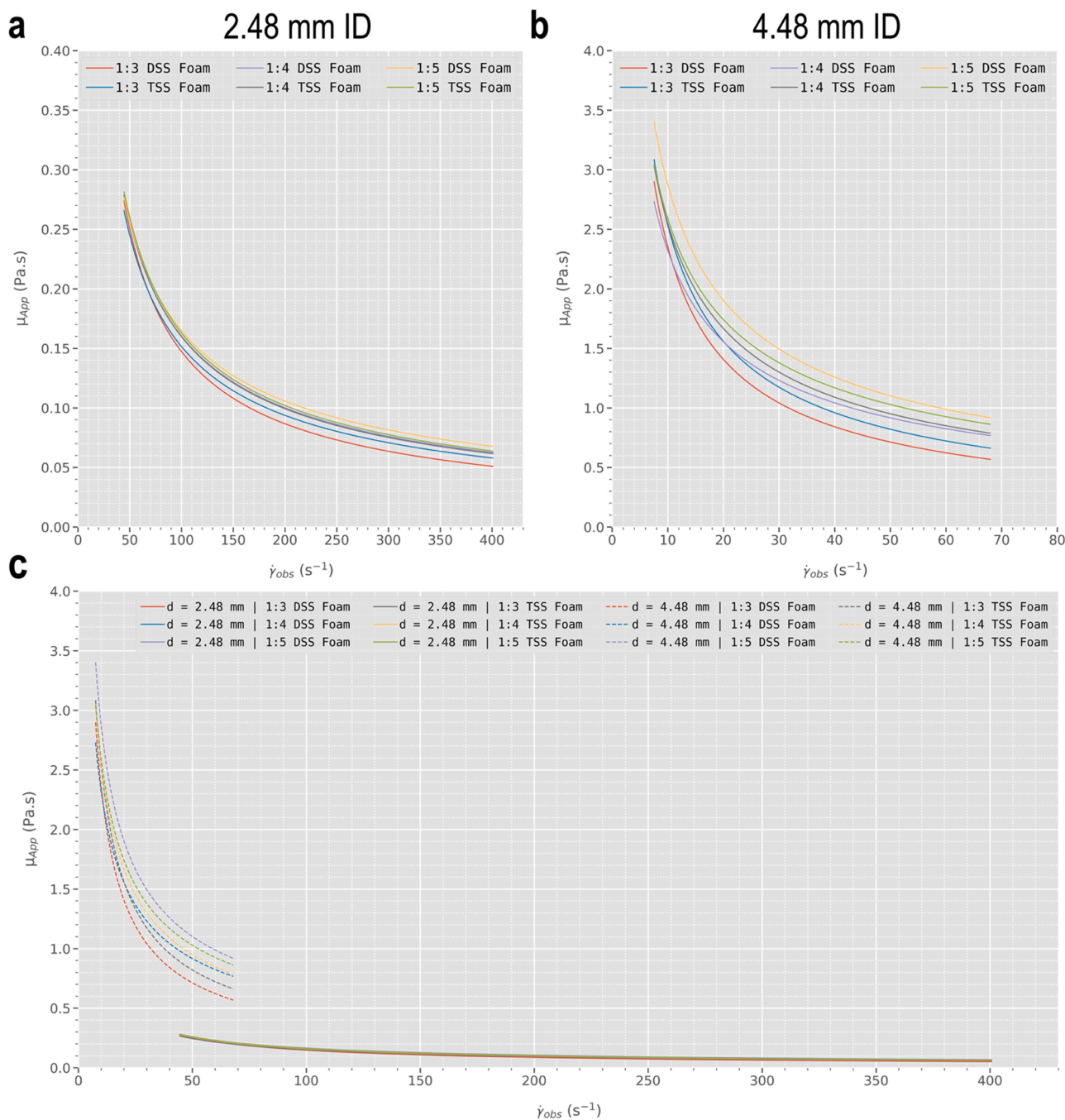


Fig. 6. Observed apparent viscosity profiles exhibited by various foams inside PTFE tubes of (a) 2.48 mm ID and (b) 4.48 mm ID. It is evident that viscosity increases with increasing the liquid-to-gas ratio, while the relative relationship among these curves seems to be preserved across different tube IDs. c) Superimposed apparent viscosity profiles of all 12 foam formulations. The segregation of viscosity profiles into two groups is due to the wall-slip phenomenon (dashed lines = 4.48 mm ID tube, solid lines = 2.48 mm ID tube).

correlated relationship between shear rate and apparent viscosity (see Eq. 5). It is important to note that, in their study of the rheology of sclerosing foams, Wong et al. eliminated wall-slip by pasting sandpaper on the walls of a rheometer, which is a widely recognised technique proposed by Khan et al. [11]. Such a method is impractical to implement on a pipe viscometer, hence the analytical Oldroyd-Jastrzebski wall-correction method was employed in the present study. It was expected for this method to yield viable correction of the wall shear stress data, given its success in previous studies on aqueous foams [9,12–14]. However, wall-slip correction in the current study was unsuccessful. The y-intercept of a $\dot{\gamma}_{obs} - 1/d^2$ graph represents observed shear rate in a tube of infinite diameter, which is interpreted as the shear associated with the

slippage effect. The negative y-intercepts in the Oldroyd-Jastrzebski graphs obtained in the present study (see Fig. 4) are thus physically meaningless. In contrast with this work, other studies in the literature succeeded at wall-slip correction of aqueous foam's rheology [9,12–14], whilst the work by Larmignat et al. on colloidal gas aphrons (a specific type of aqueous foam) found no dependence of $\dot{\gamma}_{obs}$ on $1/d^2$. Nevertheless, there are major differences among these studies in terms of the physical conditions and phenomena that potentially contribute to the slippage effect. Table 6 summarises the relevant attributes among these previous investigations, showing significant differences between the foam types used. One of the major differences between pipe viscometry of sclerosing foams described herein with other similar works is the ratio

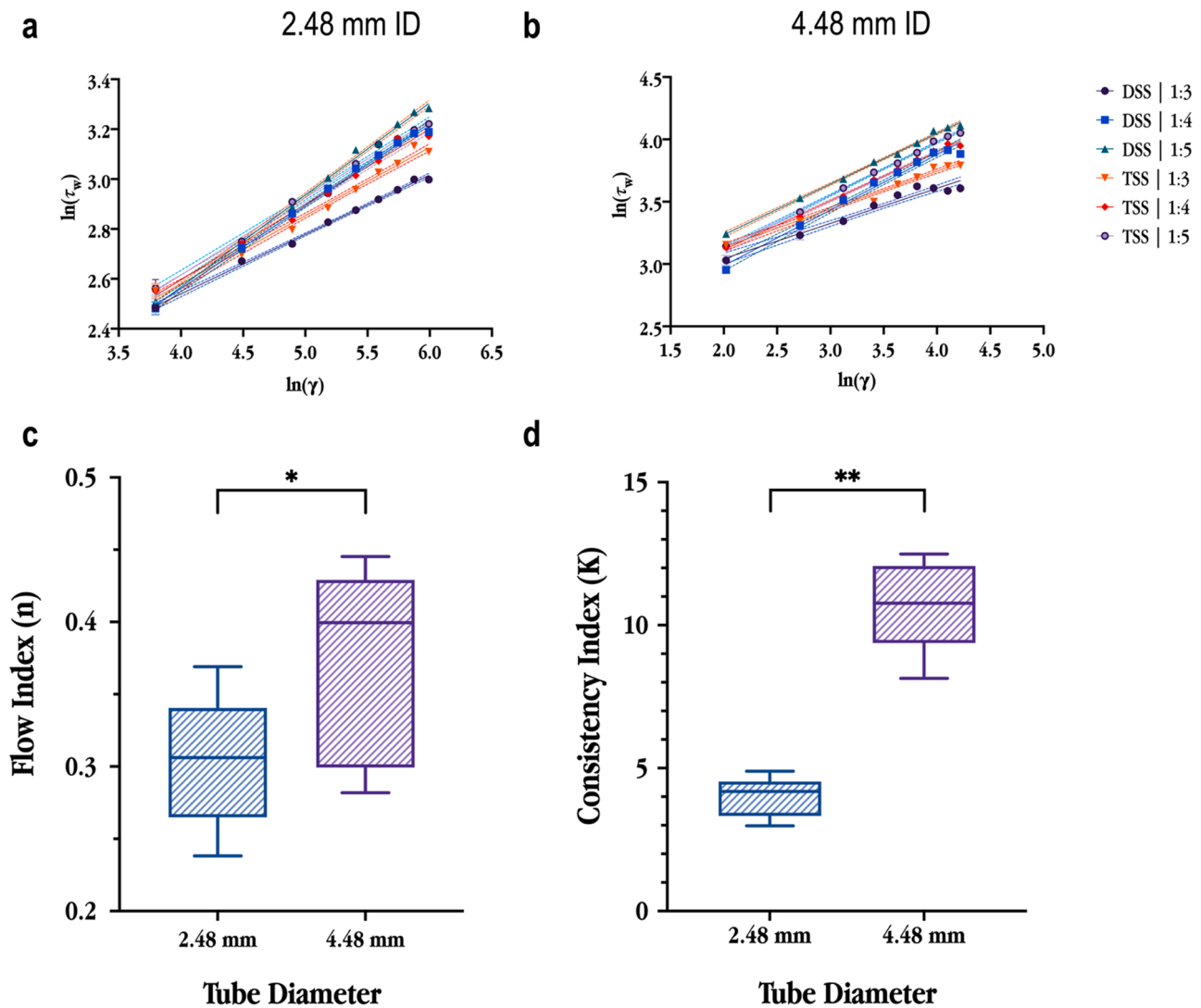


Fig. 7. Top: Regression of observed rheological data into a linearised power-law equation ($\ln \tau_w = n \ln \dot{\gamma}_{obs} + \ln K$) corresponding to (a) 2.48 mm ID and (b) 4.48 mm ID PTFE tube. Dotted lines signify a 95% confidence interval due to the error of regression. Bottom: Power-law indices of observed data. Box plots correspond to values of (c) n and (d) K , grouped with respect to tube ID (box plots show the distribution of power-law indices over the ranges of min-value, 25%, 50%, 75%, max-value). One-tailed Mann – Whitney U tests resulted in p-values of 0.0465 and 0.0011 for n and K , respectively (ns: p-value ≥ 0.05 . *: 0.01 < p-value < 0.05. **: 0.001 < p-value < 0.01. ***: p-value < 0.001).

of conduit diameter to bubble diameter ($d_{conduit}/d_{bubbles}$ – see Table 6). The largest bubbles in PCFs are approximately 510 μm and 750 μm for DSS and TSS foams, respectively. In contrast to this work, studies listed in Table 6 have all used ‘microfoams’ ($d_{bubbles} < 250 \mu\text{m}$) [27]. Consequently, since the bubble diameter of PCFs in this work is expected to be in the range 130 – 750 μm [8], bubbles are not significantly smaller than the tube IDs (with $d_{conduit}/d_{bubbles} \sim 3.3 - 34.5$), allowing the foam to behave more like a colloidal suspension of bubbles than a ‘single-phase fluid’. Additionally, all other studies use different surfactant solutions and concentrations, as well as different foaming techniques, tube materials and experimental shear rates. Failure of wall-slip correction in this work may therefore be attributed to insignificant conduit-to-bubble diameter ratios.

Another crucial variable that may affect the wall-slip phenomenon is the tube material. While other studies have used stainless steel pipes, PTFE tubes were used in this work. Furthermore, it is worth noting that during experiments, some gas bubbles would remain adhered to the tube inner walls during injection. Therefore, it is reasonable to conclude that an attractive interaction exists between the POL solution and the PTFE tube. What defines the extent of this interaction between the foam and

the tube is the wettability of PTFE, which is characterised by the contact angle of the POL solution on PTFE. The contact angle of water is $\sim 106.2^\circ$ on PTFE compared to $\sim 62.1^\circ$ on stainless steel [28]; thus, it is reasonable to conclude that these different materials may give rise to a different slippage phenomenon. Nevertheless, given the considerable difference between the surface tension of water ($\sim 72 \text{ mN/m}$) and 1% POL solutions ($\sim 24 \text{ mN/m}$) [7,29,30], the contact angle of a POL solution may largely differ from that of water and further investigations are needed to better understand the interaction of POL-based foams with different materials.

Surface properties play a role in the rheology of sclerosing foams that is yet to be fully understood. To conduct a therapeutically-relevant rheological study, it is therefore important to replicate the surface properties of the vascular endothelium. The extent of literature on such properties is limited; the only notable work [31] was carried out on rabbit arterial endothelium where the contact angle of a dextran droplet was measured within a polyethylene glycol medium (surface tension of $\sim 62 \text{ mN/m}$) and was reported to be $86^\circ \pm 11^\circ$, measured on 5 tissue samples. This calls for more extensive research to characterise the surface interaction of the vein lumen with various therapeutically-relevant

Table 2

Power-law indices obtained through regression analysis of observed $\ln \dot{\gamma}_w$ versus $\ln \dot{\gamma}_{obs}$ data using Prism. Associated standard error of means (SEMs) were automatically calculated by Prism.

#	Tube ID	Formulation	L:G ratio	n	SEM _n	K	SEM _K
1	2.48	DSS	1:3	0.2382	0.00398	4.889	0.1024
2			1:4	0.3310	0.00471	3.445	0.0854
3			1:5	0.3690	0.00588	2.977	0.0921
4		TSS	1:3	0.2738	0.00685	4.411	0.1589
5			1:4	0.3021	0.00701	4.003	0.1476
6			1:5	0.3103	0.00654	3.951	0.1360
7	4.48	DSS	1:3	0.2819	0.01369	11.93	0.5732
8			1:4	0.4453	0.01276	8.142	0.3647
9			1:5	0.4062	0.00597	11.27	0.2362
10		TSS	1:3	0.3051	0.00941	12.49	0.4126
11			1:4	0.3929	0.00647	10.27	0.2331
12			1:5	0.4237	0.00482	9.786	0.1655

Table 3

Statistical results of two-way ANOVA (p-values) conducted on observed rheological data. Results suggest that formulation technique has no interaction on the rheological behaviour of PCF sclerosing foams flowing inside larger tubes (ns: p-value ≥ 0.05 ; *: $0.01 < \text{p-value} < 0.05$; **: $0.001 < \text{p-value} < 0.01$; ***: p-value < 0.001).

	Effect of L:G ratio		Effect of Technique	
	n	K	n	K
2.48 mm	***	***	***	***
4.48 mm	***	***	ns (p = 0.62)	ns (p = 0.17)

sclerosing formulations.

Another potential consequence of bubbles adhesion over the inner surface of the PTFE tube is the reduction of effective hydraulic diameter, which in turn would decrease the calculated values of wall shear stress (see Eq. 2 and Fig. 10). Therefore, during Oldroyd-Jastrzebski construction, observed shear rate values at constant wall shear stress would be larger, which would shift the data points upwards (refer to Fig. 4). Conversely, the decrease in hydraulic diameter would also exponentially increase the x-coordinates of the Oldroyd-Jastrzebski plots ($1/d^2$), shifting the data points to the right. These counteracting effects make it difficult to predict how a reduction in hydraulic diameter would overall affect the wall-slip correction process.

4.2. Flow rheology of sclerosing foams: nominal vs. observed rheology

The flow regime of PCF foams inside the tubes was determined to be laminar, given the low Reynolds numbers ($Re < 2$ in all cases), which provides evidence in support of Eq. (1) and Eq. (2). The rheological model of sclerosing foams described in this paper has been categorised into two main subgroups: the end-effect corrected (nominal) rheology and the observed rheology. The following accounts for a comparison between these rheological models.

A clinically-relevant rheological model describes the flow behaviour of sclerosing foams upon injection into veins. Since end-effects are naturally occurring phenomena [19] in fluid flows, it is reasonable to presume their existence during sclerotherapy. This implies that a nominal rheological model may not reflect the phenomenology of foam administration in-vivo, while the observed rheological data (uncorrected for end-effects) would be more therapeutically-relevant. Although the nominal rheological behaviour of sclerosing foams may not be clinically applicable, as a physical model it remains valued. Previous

studies have demonstrated the potential of analytical pipe viscometry in developing a nominal rheological model of aqueous foams, independent of L:G ratio and tube diameter [9,13]. An attempt to further process the end-effect corrected data to develop a wall-slip corrected model was undertaken in the present study and its failure has been discussed in Section 4.1. Nevertheless, the nominal rheology of sclerosing foams through end-effect correction was successfully obtained. Whether this nominal model is clinically-relevant remains an open question, and further research would be required to validate this assumption.

The power-law indices obtained via different tube sizes differ significantly (p-value < 0.05) prior to end-effect correction ($0.238 < n < 0.369$ for the 2.48 mm tube, versus $0.282 < n < 0.445$ for the 4.48 mm tube, see Fig. 7). After end-effect correction, n values corresponding to both tubes fell within almost the same range ($0.198 < n < 0.328$ for the 2.48 mm tube, versus $0.1931 < n < 0.337$ for the 4.48 mm tube) while exhibiting an identical distribution (Fig. S10a) compared to the uncorrected n values (Fig. 7c) and no statistical difference. However, K values remained significantly different among different tubes, even after end-effect correction (see Fig. 7d and Fig. S10d). This difference is reflected in Fig. S9 where the viscosity profiles obtained via different tube diameters are shown to be different after end-effect correction, signifying the sensitivity of viscosity profiles on changes in K values.

The power-law indices of observed foam rheology were statistically analysed (see Fig. 8 and Fig. 9). A closer look at these figures suggests a lack of consistency in trends of power-law indices against different tube IDs. On the other hand, the results of nominal foam rheology (see Fig. S11 and Fig. S12) not only show a consistent correlation among power-law indices of nominal data against tube IDs, but the statistical comparisons among n values are consistent with those among K values. In other words, end-effect correction eliminated the discrepancies in trends of power-law indices among different tube IDs. This reflects the success of end-effect correction in aligning the results obtained via different tube sizes and suggests that pressure loss due to end-effects is responsible for the absence of any trend among observed power-law indices measured in tubes of different ID.

4.3. Effect of clinically-relevant parameters on sclerosing foam rheology

Presuming that during sclerotherapy, vessels experience the observed foam rheology (as opposed to the nominal rheology), the focus of this discussion will be on the observed data. The following sections account for the effects of various independent variables on the observed rheology of sclerosing foams and the corresponding implications during sclerotherapy. It is important to note that while statistical analysis reveals the significance of differences between power-law indices, it does not always translate to a statistically significant difference between viscosity profiles across the entire shear rate spectrum. It is only accurate to account two viscosity profiles significantly different if, and only if, both power-law indices are significantly different.

4.3.1. Effect of injection flowrate

In all experiments, the apparent viscosity of sclerosing foams decreased with increasing flowrate (Fig. 6), confirming their shear-thinning nature as observed in previous studies of aqueous foams [12, 15,32]. The main difference between this and previous work in this area is the use of a therapeutically-relevant viscometry technique that employs a clinical range of shear rates. Conventional rheometry of sclerosing foams conducted in previous studies employ shear rates of $0.01 - 1 \text{ s}^{-1}$ [7,15] while venous flow yields shear rates of $50 - 200 \text{ s}^{-1}$ [33, 34], which are approximately two orders of magnitude greater than those studied previously. In contrast to venous flow, the foam experiences the injection shear during administration. Lack of established guidelines on treatment injection flowrates makes it difficult to presume the injection shear rates experienced by the foam. A recent study has characterised the rate of foam expansion and formation upon immediate injection in tubes of 4 mm and 10 mm ID and has reported values of

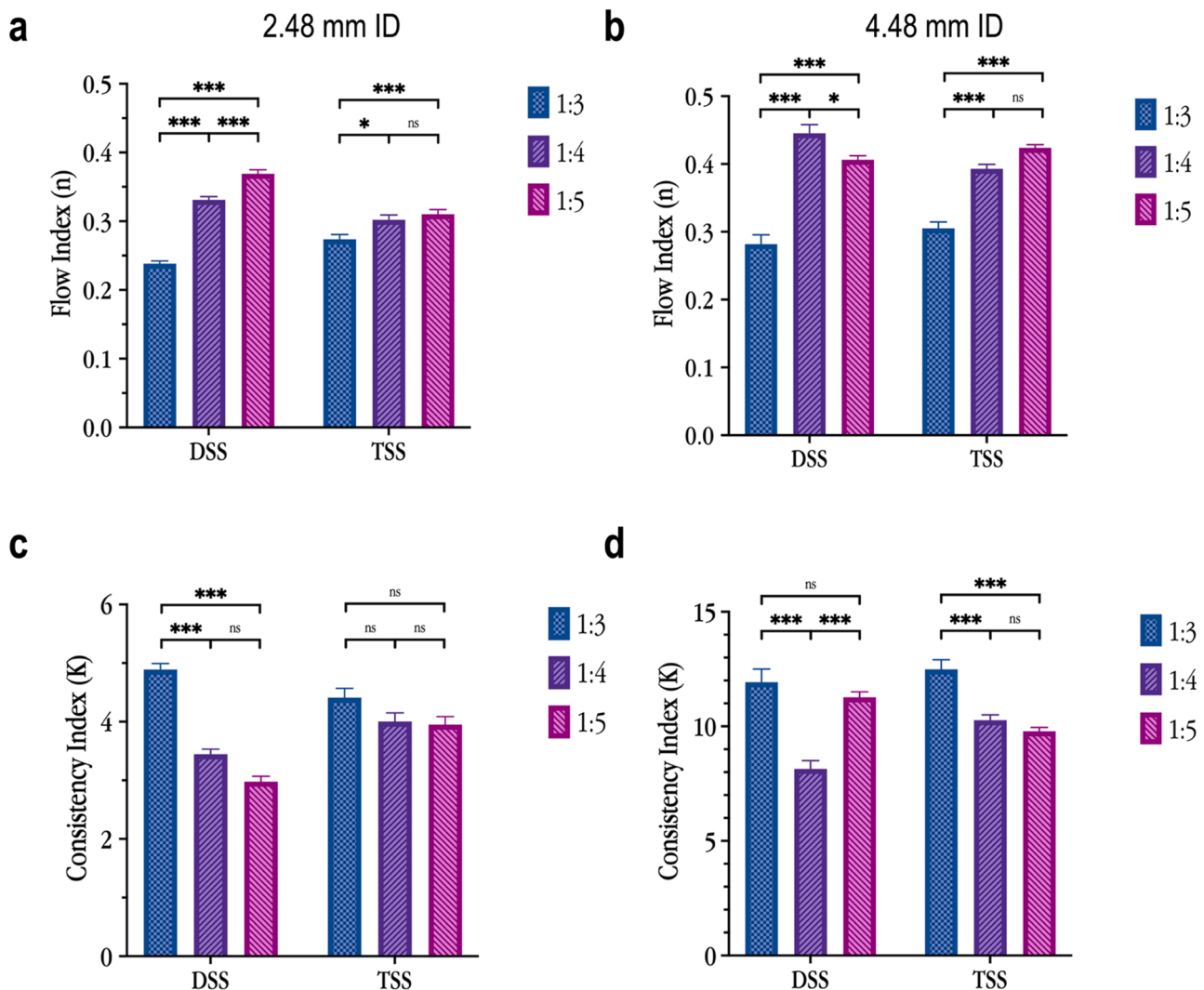


Fig. 8. Effect of L:G ratio on observed power-law indices associated with sclerosing foams produced using either the DSS or the TSS method. The top row graphs (a and b) correspond to n values, while the bottom row graphs (c and d) correspond to K values. Results of two-way ANOVA between each group of data are marked. This graph includes observed data (ns: p -value ≥ 0.05 ; *: $0.01 < p$ -value < 0.05 ; **: $0.001 < p$ -value < 0.01 ; ***: p -value < 0.001).

foam expansion rate in the range of 21 mm.s^{-1} – 52 mm.s^{-1} . Assuming that the expansion rate can be regarded as linear velocity, the flowrates employed in this previous study are in the range of $15.76 \text{ mL.min}^{-1}$ – $245.0 \text{ mL.min}^{-1}$, translating to shear rates in the range of 0.730 – 41.8 s^{-1} [5]. These values overlap with the flowrates and shear rates employed herein and verify the relevance of this work to clinical injection flowrates. Based on these considerations, it is therefore expected that apparent viscosities obtained in this work should differ from those obtained in previous studies, and yet more closely align with those likely to be observed in vivo.

Here, apparent viscosities range approximately from ~ 0.051 – 0.281 Pa.s and ~ 0.568 – 3.40 Pa.s (see Fig. 6), when measured in tube IDs of 2.48 mm (shear rates ranging ~ 44.5 – 401 s^{-1}) and 4.48 mm (shear rates ranging ~ 7.55 – 68.0 s^{-1}), respectively. Wong et al. obtained significantly different viscosity values ranging from 10 to 100 Pa.s (measured via cone-plate rheometry), which are several orders of magnitude greater than those obtained in this work. This may be due to the much smaller shear rates applied in their work compared to those employed herein and is in fact in agreement with the shear-thinning behaviour of aqueous foams [7]. In contrast to Wong et al., the findings by Critello et al. are in close agreement with this work [15], although the employed shear rates are different to those applied here. Critello et al. utilised cone-plate viscometry of 1:5 (L:G ratio) POL foams

to obtain viscosity values ranging approximately from 0.05 to 0.250 Pa.s , measured under shear rates of 0.01 – 0.1 s^{-1} . Nevertheless, major differences exist between the experimental conditions of Critello et al. and Wong et al.; the most important of which is the absence of any wall-slip elimination mechanism in Critello's work. Additionally, Critello et al. employed POL solutions with concentrations below 0.5%, which could explain the relatively smaller reported viscosity values. In conclusion, the works of Wong et al. and Critello et al. utilise experimental conditions and apparatuses that are different to those employed in this work. Given the shear-history sensitivity of aqueous foam rheology, it can be inferred that the results of conventional rheometry cannot be used to predict therapeutic efficacy.

4.3.2. Effect of vessel size

The viscosity profiles obtained in different tube sizes yielded largely different results. The Mann-Whitney test (Fig. 7) confirms a significant difference between both power-law indices (K and n) obtained using different pipe diameters. The dependence of foam rheology on tube diameter is thus confirmed with at least 95% confidence (see Fig. 7). In the smaller tube n and K values ranged from 0.238 to 0.369 and 2.98 – 4.89, compared to 0.282 – 0.445 and 8.14 – 12.5 obtained from the larger tube. K values remained statistically different after end-effect correction; thus, it can then be concluded with certainty that wall-slip

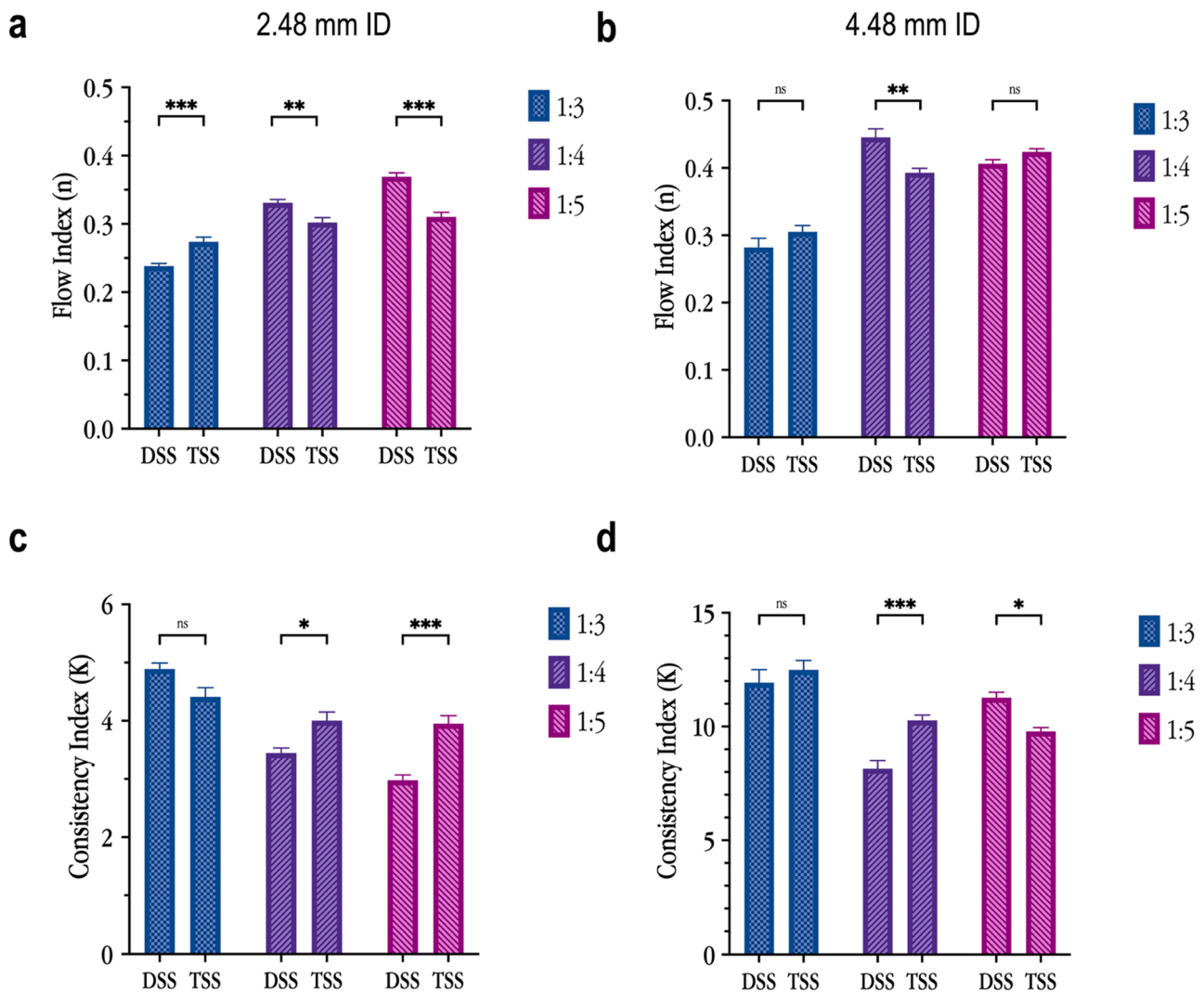


Fig. 9. Effect of formulation technique on observed power-law indices associated with sclerosing foams produced using different L:G ratios. The top row graphs (a and b) correspond to n values while the bottom row graphs (c and d) correspond to K values. Results of two-way ANOVA between each group of data are marked. This graph includes observed data (ns: p -value ≥ 0.05 . *: $0.01 < p$ -value < 0.05 . **: $0.001 < p$ -value < 0.01 . ***: p -value < 0.001).

Table 4

Summary of statistical results (two-way ANOVA) corresponding to the comparison of different formulation techniques and the resulting impact on the level of statistical significance associated with comparing apparent viscosity (μ_{app}) profiles (ns: p -value ≥ 0.05 . *: $0.01 < p$ -value < 0.05 . **: $0.001 < p$ -value < 0.01 . ***: p -value < 0.001).

Vessel Size	Technique Comparing	L:G ratio	n	K	μ_{app}
2.48 mm	DSS vs. TSS	1:3	***	ns	Not necessarily significant
		1:4	**	*	Significant
		1:5	***	***	Significant
4.48 mm	DSS vs. TSS	1:3	ns	ns	Not significant
		1:4	**	***	Significant
		1:5	ns	*	Not necessarily significant

is a critical factor that defines the flow behaviour of foam depending on conduit diameter.

The μ_{app} profiles experienced by the 4.48 mm ID pipe viscometer are about one order of magnitude greater than those observed using the 2.48 mm ID tube (see Fig. 6). Additionally, the smaller tube experiences

a narrower range of viscosities. This therefore implies that sclerosing foam rheology may not play a significant role in the flow behaviour of foams in smaller veins (ID $< \sim 2.5$ mm). On the other hand, larger vessels (ID $> \sim 2.5$ mm) experience a rather greater range of viscosities under variable injection rates, thus injection flowrate must be considered a crucial variable in the treatment of larger vessels and needs to be characterised accordingly.

To evaluate the extent of interaction between formulation parameters and foam rheology, two-way ANOVA tests were conducted on the power-law indices. It was revealed that both L:G ratio and the type of manual formulation technique impact on the overall rheology of foam with great significance ($> 99.9\%$) among almost all experimental conditions. The exception is the independence of foam rheology and the utilised formulation technique in the larger tube (see Table 3). This may imply a lower significance of the type of manual formulation technique used on foam rheology when treating larger veins (ID $> \sim 2.5$ mm).

4.3.3. Effect of foam formulation

Results show that apparent viscosity increases with L:G ratio. This trend is observed in results obtained with both tube sizes and corroborates previous findings on rheology of other aqueous foam types [12, 13], as well as those obtained on sclerosing foams [7,15]. The effect of formulation technique seems to be arbitrary, nevertheless, it appears

Table 5

Summary of statistical results (two-way ANOVA) corresponding to the comparison of different formulation techniques and L:G ratios, and the resulting impact on the level of statistical significance associated with comparing apparent viscosity (μ_{app}) profiles (ns: p-value ≥ 0.05 . *: $0.01 < \text{p-value} < 0.05$. **: $0.001 < \text{p-value} < 0.01$. ***: p-value < 0.001).

Vessel Size	Technique	L:G ratio Comparing	n	K	μ_{app}
2.48 mm	DSS	1:3 vs. 1:4	***	***	Significant
		1:3 vs. 1:5	***	***	Significant
		1:4 vs. 1:5	***	ns	Not necessarily significant
	TSS	1:3 vs. 1:4	*	ns	Not necessarily significant
		1:3 vs. 1:5	***	ns	Not necessarily significant
		1:4 vs. 1:5	ns	ns	Not significant
		1:3 vs. 1:4	***	***	Significant
		1:3 vs. 1:5	***	ns	Not necessarily significant
4.48 mm	DSS	1:4 vs. 1:5	*	***	Significant
		1:3 vs. 1:4	***	***	Significant
	TSS	1:3 vs. 1:5	***	***	Significant
		1:4 vs. 1:5	ns	ns	Not significant

that wetter (1:3) DSS foams are less viscous than wetter (1:3) TSS foams, whereas drier (1:5) DSS foams are more viscous than drier (1:5) TSS foams. The viscosity of 1:4 foams is very similar between the two formulation methods (see Fig. 6). Furthermore, it is evident that TSS foams of different L:G ratios exhibit near-identical viscosities in the smaller tube (Fig. 6a). This implies that the DSS formulation technique would generally yield foams with more diverse rheological characteristics relative to TSS foams, under varying L:G ratio formulations. In other words, the rheological characteristics of DSS foams are seemingly more sensitive to L:G ratio.

It can be inferred from Table 4 that formulation technique has negligible impact on the rheology of wetter (1:3) PCF foams while drier foams are more prone to rheological variation due to varying formulation techniques, especially inside narrower conduits. Consequently, formulation technique may not be of clinical importance when administering wetter PCF foams in smaller veins ($ID \leq \sim 2.5$ mm). A comparison of the individual results of different L:G ratios across different formulation techniques and different vessel sizes reveals that DSS and TSS foams of 1:3 and 1:5 L:G ratio may behave similarly, whereas 1:4 DSS foams are significantly different (less viscous) compared to 1:4 TSS foams. It can then be concluded that the only statistically significant difference among power-law indices that reflects a distinct viscosity

variation in any vessel size is between drier (1:4) TSS and DSS foams.

Viscosity profiles are more spread out when measured in the larger tube (in agreement with more statistical significance among data from the large tube), which can be attributed to greater slippage experienced by the foam in the larger tube; nevertheless, viscometry in both tubes yielded very similar trends with respect to foam L:G ratio. However, statistical tests show that the manual formulation technique used has no significant impact on the rheology of PCF foams injected into larger vessels; therefore, it may not be a relevant factor when treating larger veins ($ID > \sim 2.5$ mm). Furthermore, as discussed above, the DSS technique yields a greater spread in apparent viscosity profiles of foams formulated using different L:G ratios compared to TSS, and this spread is more pronounced in the larger tube. This observation is reflected in the two-way ANOVA results (Table 5) where there is no significant difference between K values of TSS foams in the smaller tube (3.9, 4.0 and 4.4), in contrast to significant differences among K values of TSS foams obtained from the larger tube (9.8, 10.3 and 12.5). The overall results indicate that there is a directly proportional relationship between gas fraction and foam viscosity, with DSS yielding stronger statistical evidence inside smaller vessels. The potential clinical implications of these results are discussed in Section 4.5.

4.4. Variation of foam viscosity during injection

As described in Section 2.3.1, pressure curves exhibited diverse profiles across different injection flowrates (see Section 2.2.1 and Fig. S3). Notably, pressure curves showed a decline after the ΔP plateaued during slower injections. This decline in pressure differential can

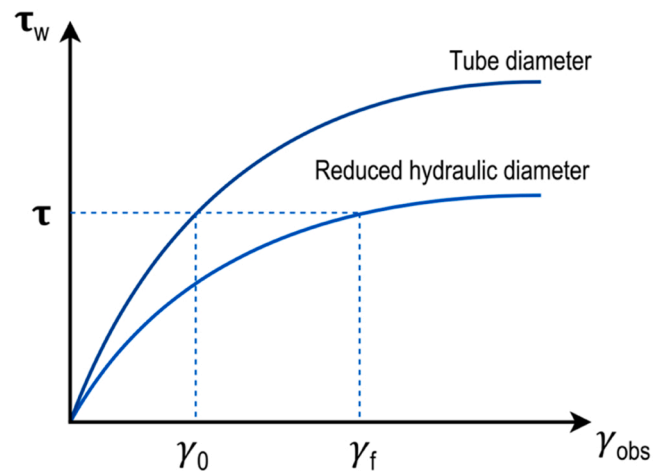


Fig. 10. A reduction in hydraulic diameter would yield a decrease in calculated wall shear stress values. Consequently, the observed shear rate at a constant wall shear stress value would increase.

Table 6

Summary of the differences between experimental conditions and fluid properties among studies on rheological characterisation of aqueous foams that utilise analytical methods of wall-slip correction. POL: polidocanol; SDS: sodium dodecyl sulfate.

Attribute	This work	Bekkour et al.	Gardiner et al.	Enzendorfer et al.	Herzhaft et al.
Foam Type	POL foams	SDS foams	Ether sulphate foams	Hydroxypropylguar foamed polymer solution	Hydroxypropylguar foamed polymer solution
Production Technique	PCF (DSS and TSS)	Packed bed foam generator	Mixing with Compressed Air	Packed bed foam generator	Packed bed foam generator
Rheometry Method	PTFE Pipe Viscometry	Controlled Stress Rheometry	Stainless Steel Pipe Viscometry	Stainless Steel Pipe Viscometry	Stainless Steel Pipe Viscometry
Conduit Width ($d_{conduit}$) /mm	2.48 – 4.48	60	6.95 – 15.8	4.05 – 12.0	7.7 – 10.9
Bubble Size ($d_{bubbles}$) / μm	130 – 750 (Carugo et al., 2016)	200	100	Not specified, but deemed negligible compared to conduit diameter	10 – 90
$d_{conduit}/d_{bubbles}$ ratio	3.3 – 34.5	30,000	69.5 – 158.0	$\approx \infty$	85.6 – 726.7
Range of shear rates	$\approx 7 - 400 \text{ s}^{-1}$	$0 - 350 \text{ s}^{-1}$	$64 - 3340 \text{ s}^{-1}$	$3 - 2500 \text{ s}^{-1}$	$0.1 - 1000 \text{ s}^{-1}$

be attributed to the ageing phenomenon occurring throughout the course of injection. In principle, the longer it takes for the foam to be completely injected into the viscometer, the more time there is for drainage and bubble coarsening and coalescence to occur. Therefore, the foam evolves during injection and, consequently, ΔP could vary over time. In this work, the slowest injection ($4.00 \text{ mL} \cdot \text{min}^{-1}$) would take 2 min, while the fastest injection ($36.0 \text{ mL} \cdot \text{min}^{-1}$) would take less than 14 s. Given that the half-lives¹ of polidocanol-based DSS and TSS foams are 160 and 90 s [8], it is safe to presume that the slowest injection rates employed in this work provide sufficient residence times for sclerosing foams to age within the pipe viscometer. Thus, this time-dependent nature of the foam structure implies that under slower injection rates, foam viscosity inevitably evolves over the course of injection.

While stationary aqueous foams experience drainage, flowing foams could experience an emphasised drainage effect due to shear; yet this has not been addressed extensively in the literature. Goyon et al. investigated the drainage of tetradecyl trimethyl ammonium bromide foams using magnetic resonance imaging (MRI) while being sheared in a Couette rheometer, and have reported on the effects of bubble size and surfactant mobility at the gas-liquid interface [35]. Their results show that the rate of drainage for sheared monodisperse foams increases by a factor of 1.5 when increasing bubble size from $125 \mu\text{m}$ to $500 \mu\text{m}$. They have established a direct correlation between bubble size and shear-induced drainage whereby foams with smaller bubble sizes were shown to drain much faster. Goyon et al. validated the presence of shear-induced drainage, but its interaction with the rheological behaviour of foams was not investigated. Moreover, such studies have never been conducted on sclerosing foams and given the dependence of interface mobility on surfactant chemistry, it is difficult to employ these earlier investigations to predict shear-induced drainage of sclerosing foams.

The large inner diameter of the 10 mL syringe used here ($ID = 15.96 \text{ mm}$) would result in a maximum shear rate of 1.50 s^{-1} inside the syringe (at $36.0 \text{ mL} \cdot \text{min}^{-1}$), while the maximum shear rate within the entire pipe viscometry apparatus (401 s^{-1}) occurs inside the 2.48 mm tube at $36.0 \text{ mL} \cdot \text{min}^{-1}$. Consequently, the syringe is expected to play little part in contributing to shear-emphasised drainage effects. If anything, shear-induced drainage should be most prominent in the 2.48 mm tube. Considering that DSS (foam half-life: 160 s) is much more stable than TSS (foam half-life: 90 s), it is expected for TSS foam to exhibit a greater variation in viscosity over time due to quasi-static drainage. Another factor that derives from the ageing phenomenon, is bubble coarsening (otherwise known as Ostwald ripening), which governs the evolution of bubble sizes via diffusion of gas from high-pressure smaller bubbles to low-pressure larger bubbles driven by Laplace pressure. Ostwald ripening occurs more rapidly in foams with a wider bubble size distribution [36,37]. Given that TSS foams exhibit a wider bubble size distribution as well as a shorter half-life [8], they are expected to show the greatest ageing-related variation in rheological behaviour. This prediction is not verified in this work as the min-max regions of DSS rheograms are very similar to those of TSS foams (see Fig. S5 and Fig. S6). In conclusion, dedicated experiments need to be designed in the future to extensively evaluate the correlation between shear-induced ageing and rheology of sclerosing foams.

4.5. Clinical predictions

To formulate clinical predictions, an assumption must be made regarding the effect of sclerosing foam rheology on the biological outcomes of treatment. Greater foam viscosity could result in a more cohesive foam plug, which could in turn yield more optimum blood displacement by the foam and could mean a greater foam dwell time [5].

Thus, assuming a direct correlation, i.e., higher viscosity ultimately leads to better treatment outcomes, it is possible to develop specific arguments regarding the clinical significance of the rheological results. This assumption shall be referred to as the “viscous-desirability assumption” henceforth. The authors aim to evaluate this assumption in future studies by correlating foam rheology with clinically-relevant parameters.

Following the viscous-desirability assumption, it can be inferred that lower injection flowrates would ultimately lead to better treatment outcomes, especially when treating larger veins as the observed apparent viscosities are shown to be greater inside wider conduits. It is also worth noting that employing lower flowrates may result in inconsistent foam viscosities, especially when treating larger veins where foam rheology is more sensitive to ageing and variations in L:G ratio. Additionally, there appears to be no significant difference between PCF formulations when treating larger veins ($ID > \sim 2.5 \text{ mm}$). Given the dilated morphology of varicose veins, it can be concluded that there exists no rheologically optimal PCF formulation technique for the treatment of varicose veins if the target vessels are larger than $\sim 2.5 \text{ mm}$ in diameter. For varicose veins smaller than $\sim 2.5 \text{ mm}$, no optimal manual formulation technique exists for 1:3 and 1:4 foams (both PCFs perform similarly), while DSS is expected to yield more favourable therapeutic outcomes when using 1:5 foams. Previous studies have evaluated the therapeutic efficacy of sclerosing foams *in vitro* and *ex vivo*. These works demonstrated the superiority of the DSS formulation technique in detaching endothelial cells and initiating apoptosis [4,38]. These findings are partially in agreement with the results of this work, though they lack data on the correlation between L:G ratio and therapeutic efficacy.

5. Conclusions

We report on a therapeutically-relevant rheometry technique to characterise the observed and nominal rheology of sclerosing foams, to better understand their flow behaviour during a typical sclerotherapy treatment of varicose veins. We applied robust statistical methods to evaluate the dependency of sclerosing foam rheology on a range of independent variables (i.e., injection flowrate, formulation technique and L:G ratio). In contrast with previous research that utilises conventional rheometry, the novel approach employed herein more closely mimics the geometrical and physical conditions of foam administration. The resultant rheological model and findings can therefore contribute towards optimising the formulation and administration techniques of sclerotherapy. Notably, pipe viscometry was successful at obtaining relevant rheological data that were fitted into a power-law model to find the power-law indices (n and K). Analytical end-effect correction (the Bagley method) was applied on the observed rheological behaviour of sclerosing foams, resulting in the nominal (end-effect independent) rheology. Wall-slip correction (Oldroyd-Jastrzebski method) was attempted but was not successful. The underlying reasons contributing to the failure of wall-slip correction are unclear and require further experimentation, although it is hypothesised that tube material, bubble size, and adhesion of bubbles to the tube walls may play critical roles in the mechanism of foam-tube interaction. Although a nominal rheological model of sclerosing foams is a valuable contribution, its utility in clinical applications is open to interpretation due to the presence of end-effects during foam administration which would give precedence to the observed rheological model. As a result, the focus of this study has been on the observed rheological model of sclerosing foams.

The shear-thinning behaviour of PCF sclerosing foams was verified and the effects of L:G ratio and formulation technique were characterised. Apparent viscosity of foam was found to be ranging from $\sim 0.051\text{--}0.281 \text{ Pa} \cdot \text{s}$ and $0.568\text{--}3.40 \text{ Pa} \cdot \text{s}$, measured in the small tube ($ID = 2.48 \text{ mm}$, shear rates ranging $\sim 44.5\text{--}401 \text{ s}^{-1}$) and the large tube ($ID = 4.48 \text{ mm}$, shear rates ranging $7.55\text{--}68.0 \text{ s}^{-1}$), respectively. Other studies on sclerosing foam rheology report significantly different values,

¹ Half Life: Time required for half of the liquid content of an aqueous foam to drain.

although the experimented shear rates and the apparatuses employed are significantly different compared to this work, making a direct comparison of results impossible. Nevertheless, this work models sclerosing foam rheology under conditions that more closely mimic their end-point application instead of employing conventional rheometry techniques that are not therapeutically-relevant in nature.

It was shown that foam viscosity increases with increasing gas fraction; i.e. the drier the foam, the greater its viscosity. The type of manual formulation technique was shown to make no significant difference to foam rheology in conduits with ID > 2.5 mm, while in smaller conduits (ID ≤ 2.5 mm) it was a defining variable. Additionally, TSS foams of different L:G ratios exhibited a narrower range of viscosity profiles in both conduits in comparison with DSS foams, implying that DSS foams could potentially yield more rheologically diverse foams. Furthermore, statistical analysis of results revealed that formulation technique does not affect the rheology of wetter (1:3) PCF foams while drier (1:5) PCF foams may exhibit significantly different rheologies when formulated using different techniques.

The observed rheology of foam was also dependent on conduit diameter, although this dependency was reduced upon end-effect correction. The observed viscosities were within a broader range in the larger conduit, implying a greater variation in foam rheology in larger vessels (ID > 2.5 mm). Additionally, apparent viscosity profiles were about an order of magnitude greater when measured in the larger vessel, demonstrating the dependence of foam rheology on conduit diameter.

While the viscosity of sclerosing foams has been thoroughly characterised, its relationship to therapeutic outcomes remains unclear. If higher viscosity translates to a more cohesive and stable foam plug, it can be inferred that this could also lead to a greater dwell time and therefore better treatment outcomes and lower recurrence rates. Following this assumption, the following conclusions can be drawn from the present study:

- Formulation technique of physician-compounded foams should not affect treatment outcomes in smaller vessels (ID ≤ 2.5 mm), especially when using wetter (1:3) foams.
- Lower injection flowrates and drier foams should improve outcomes.
- When employing drier (1:5) foams, the DSS technique is predicted to improve treatment efficacy compared to the Tessari method.
- Wetter (1:3 and 1:4) foams formulated via the Tessari method should yield better outcomes compared to the DSS method.
- If the TSS method is used, the L:G ratio should make no significant difference in treatment outcomes.

In conclusion, pipe viscometry not only proved highly efficient in modelling the rheological behaviour of sclerosing foams in a therapeutically-relevant setting, but it also led to complications due to tube material properties, creating discrepancies in the Oldroyd-Jastrzebsky plots (namely the negative y-intercepts) that ultimately rendered wall-correction physically meaningless. Although the correction methods may not be relevant to clinical therapies, they remain valuable tools for characterisation of nominal foam rheology. Failure of wall-slip correction provided an opportunity to question the surface interaction between conduit material and foam. Thus, the characterisation of surface properties of the vessels with respect to sclerosing foams appears to be an important gap in the literature. The results of this work will be used in future experiments of sclerosing foams to determine the most optimal foam formulation for the treatment of varicose veins.

CRediT authorship contribution statement

Alireza Meghdadi: performed all experiments and data analyses in this study, wrote and revised the paper. **Stephen A. Jones** and **Venisha A. Patel**: provided feedback throughout the research project, and revised the paper. **Andrew L. Lewis** and **Timothy M. Millar**: co-supervised the research project and revised the paper. **Dario Carugo**: developed the research project, primary project supervisor, and revised the paper.

Declaration of Competing Interest

The authors declare the following financial interests/personal relationships which may be considered as potential competing interests: **Stephen A. Jones**, **Venisha A. Patel** and **Andrew L. Lewis** were employees at Biocompatibles Ltd. (a BTG International group company), and were working on the development of Varithena™. **Alireza Meghdadi's** PhD research project at the University of Southampton was partially funded by BTG International.

Acknowledgements

The authors would like to thank BTG International Ltd. and the UK Engineering and Physical Sciences Research Council (EPSRC; i.e. through a Doctoral Training Partnership, DTP) for funding Alireza Meghdadi's PhD research project and studentship.

Appendix A. Supporting information

Supplementary data associated with this article can be found in the online version at doi:10.1016/j.colsurfa.2022.128916.

References

- [1] E. Cameron, T. Chen, D.E. Connor, M. Behnia, K. Parsi, Sclerosant foam structure and stability is strongly influenced by liquid air fraction, *Eur. J. Vasc. Endovasc. Surg.* 46 (4) (2013) 488–494, <https://doi.org/10.1016/j.ejvs.2013.07.013>.
- [2] T. Bai, et al., A review of sclerosing foam stability in the treatment of varicose veins, *Dermatol. Surg.* 46 (2) (2020) 249–257, 2020.
- [3] T. Bai, W. Jiang, Y. Chen, F. Yan, Z. Xu, Y. Fan, Effect of multiple factors on foam stability in foam sclerotherapy, *Sci. Rep.* 8 (1) (2018) 15683, <https://doi.org/10.1038/s41598-018-33992-w>.
- [4] E. Bottaro, et al., Physical vein models to quantify the flow performance of sclerosing foams, *Front. Bioeng. Biotechnol.* 7 (2019) 2019, <https://doi.org/10.3389/fbioe.2019.00109>.
- [5] D. Carugo, et al., The role of clinically-relevant parameters on the cohesiveness of sclerosing foams in a biomimetic vein model, *J. Mater. Sci. Mater. Med.* 26 (11) (2015) 2015, <https://doi.org/10.1007/s10856-015-5587-z>.
- [6] V. Nastasa, et al., Properties of polidocanol foam in view of its use in sclerotherapy, *Int. J. Pharm.* 478 (2) (2015) 588–596, <https://doi.org/10.1016/j.ijpharm.2014.11.056>.
- [7] K. Wong, T. Chen, D.E. Connor, M. Behnia, K. Parsi, Basic physicochemical and rheological properties of detergent sclerosants, *Phlebology* 30 (5) (2015) 339–349, <https://doi.org/10.1177/0268355514529271>.
- [8] D. Carugo, et al., Benefits of polidocanol endovenous microfoam (Varithena®) compared with physician-compounded foams, *Phlebology* 31 (4) (2016) 283–295, <https://doi.org/10.1177/0268355515589063>.
- [9] C. Enzendorfer, R.A. Harris, P. Valkó, M.J. Economides, P.A. Fokker, D.D. Davies, Pipe viscometry of foams, *J. Rheol.* 39 (2) (2002) 345–358, <https://doi.org/10.1122/1.550701>.
- [10] N.D. Denkov, V. Subramanian, D. Gurovich, A. Lips, Wall slip and viscous dissipation in sheared foams: effect of surface mobility, (in English), *Colloid Surf. A* 263 (1–3) (2005) 129–145, <https://doi.org/10.1016/j.colsurfa.2005.02.038>.
- [11] S.A. Khan, C.A. Schnepfer, R.C. Armstrong, Foam rheology: III. Measurement of shear flow properties, *J. Rheol.* 32 (1) (1988) 69–92, <https://doi.org/10.1122/1.549964>.
- [12] K. Bekkour, O. Scriven, Time-dependent and flow properties of foams, *Mech. Time Depend. Mater.* (1998), <https://doi.org/10.1023/A:1009841625668>.

- [13] B.S. Gardiner, B.Z. Dlugogorski, G.J. Jameson, Rheology of fire-fighting foams, *Fire Saf. J.* 31 (1) (1998) 61–75, [https://doi.org/10.1016/S0379-7112\(97\)00049-0](https://doi.org/10.1016/S0379-7112(97)00049-0).
- [14] B. Herzhaft, S. Kakadjian, M. Moan, Measurement and modeling of the flow behavior of aqueous foams using a recirculating pipe rheometer, 2005, vol. 263, pp. 153–164, doi: [10.1016/j.colsurfa.2005.01.012](https://doi.org/10.1016/j.colsurfa.2005.01.012).
- [15] C.D. Critello, A.S. Fiorillo, M.C. Cristiano, S. de Franciscis, R. Serra, Effects of sulodexide on stability of sclerosing foams, *Phlebology* 34 (3) (2019) 191–200, <https://doi.org/10.1177/0268355518779844>.
- [16] S. Larmignat, D. Vanderpool, H.K. Lai, L. Pilon, Rheology of colloidal gas aphrons (microfoams), *Colloids Surf. A Physicochem. Eng. Asp.* 322 (1–3) (2008) 199–210, <https://doi.org/10.1016/j.colsurfa.2008.03.010>.
- [17] H. Tseng, L. Pilon, G.R. Warrier, Rheology and convective heat transfer of colloidal gas aphrons in horizontal mini-channels, *Int. J. Heat. Fluid Flow* 27 (2) (2006) 298–310, <https://doi.org/10.1016/j.ijheatfluidflow.2005.08.009>.
- [18] P. Valkó, M.J. Economides, Volume equalized constitutive equations for foamed polymer solutions, *J. Rheol.* 36 (6) (2002) 1033–1055, <https://doi.org/10.1122/1.550300>.
- [19] A.M. Rao, *Rheology of fluid, semisolid, and solid foods. Principles and Applications*, third ed., Springer, 2014.
- [20] J. Aho, S. Syrjäälä, Determination of the entrance pressure drop in capillary rheometry using Bagley correction and zero-length capillary, *Annu. Trans. Nord. Rheol. Soc.* 14 (2006), 2006.
- [21] C. Hamel-Desnos, et al., Comparison of 1% and 3% polidocanol foam in ultrasound guided sclerotherapy of the great saphenous vein: a randomised, double-blind trial with 2 year-follow-up. The 3/1 Study, *Eur. J. Vasc. Endovasc. Surg.* 34 (6) (2007) 723–729, <https://doi.org/10.1016/j.ejvs.2007.07.014>.
- [22] T. Yamaki, M. Nozaki, H. Sakurai, M. Takeuchi, K. Soejima, T. Kono, Multiple small-dose injections can reduce the passage of sclerosant foam into deep veins during foam sclerotherapy for varicose veins, *Eur. J. Vasc. Endovasc. Surg.* 37 (3) (2009) 343–348, <https://doi.org/10.1016/j.ejvs.2008.08.021>.
- [23] C. Hamel-Desnos, et al., Evaluation of the efficacy of polidocanol in the form of foam compared with liquid form in sclerotherapy of the greater saphenous vein: initial results, *Dermatol. Surg.* 29 (12) (2003) 1170–1175, <https://doi.org/10.1111/j.1524-4725.2003.29398.x>.
- [24] L. Tessari, A. Cavezzi, A. Frullini, Preliminary experience with a new sclerosing foam in the treatment of varicose veins, *Dermatol. Surg.* 27 (1) (2001) 58–60, <https://doi.org/10.1046/j.1524-4725.2001.00192.x>.
- [25] N.J. Alderman, *Non-Newtonian Fluids: Tube Viscometry - Worked Example*, 2004 ed: Engineering Sciences Data Unit, 2004.
- [26] A. Meghdadi, S.A. Jones, V.A. Patel, A.L. Lewis, T.M. Millar, D. Carugo, Foam-in-vein: a review of rheological properties and characterization methods for optimization of sclerosing foams, (in en), *J. Biomed. Mater. Res. Part B Appl. Biomater.* 109 (1) (2021) 69–91, <https://doi.org/10.1002/jbm.b.34681>.
- [27] Y. Sun, et al., Bleomycin Polidocanol Foam (BPF) stability - in vitro evidence for the effectiveness of a novel sclerosant for venous malformations, *Eur. J. Vasc. Endovasc. Surg.* 59 (6) (2020) 1011–1018, <https://doi.org/10.1016/j.ejvs.2020.01.023>.
- [28] A. Martínez-Urrutia, P. Fernandez de Arroiabe, M. Ramirez, M. Martínez-Agirre, M. Mounir Bou-Ali, Contact angle measurement for LiBr aqueous solutions on different surface materials used in absorption systems, *Int. J. Refrig.* 95 (2018) 182–188, <https://doi.org/10.1016/j.ijrefrig.2018.05.041>.
- [29] I.M. Hauner, A. Deblais, J.K. Beattie, H. Kellay, D. Bonn, The dynamic surface tension of water, *J. Phys. Chem. Lett.* 8 (7) (2017) 1599–1603, <https://doi.org/10.1021/acs.jpclett.7b00267>.
- [30] G.C. Valenzuela, K. Wong, D.E. Connor, M. Behnia, K. Parsi, Foam sclerosants are more stable at lower temperatures, *Eur. J. Vasc. Endovasc. Surg.* 46 (5) (2013) 593–599, <https://doi.org/10.1016/j.ejvs.2013.08.012>.
- [31] J.F. Boyce, P.C. Wong, S. Schurch, M.R. Roach, Rabbit arterial endothelium and subendothelium. A change in interfacial free energy that may promote initial platelet adhesion, *Circ. Res.* 53 (3) (1983) 372–377, <https://doi.org/10.1161/01.RES.53.3.372>.
- [32] S. Cohen-Addad, R. Höhler, O. Pitois, Flow in foams and flowing foams, *Annu. Rev. Fluid Mech.* 45 (1) (2013) 241–267, <https://doi.org/10.1146/annurev-fluid-011212-140634>.
- [33] J.J. Hathcock, Flow effects on coagulation and thrombosis, *Arterioscler. Thromb. Vasc. Biol.* 26 (8) (2006) 1729–1737, <https://doi.org/10.1161/01.ATV.0000229658.76797.30>.
- [34] X. Shi, et al., Effects of different shear rates on the attachment and detachment of platelet thrombi, *Mol. Med. Rep.* 13 (3) (2016) 2447–2456, <https://doi.org/10.3892/mmr.2016.4825>.
- [35] J. Goyon, F. Bertrand, O. Pitois, G. Ovarlez, Shear induced drainage in foamy yield-stress fluids, *Phys. Rev. Lett.* 104 (12) (2010), <https://doi.org/10.1103/PhysRevLett.104.128301>.
- [36] S.A. Magrabi, B.Z. Dlugogorski, G.J. Jameson, Bubble size distribution and coarsening of aqueous foams, (in English), *Chem. Eng. Sci.* 54 (18) (1999) 4007–4022, [https://doi.org/10.1016/s0009-2509\(99\)00098-6](https://doi.org/10.1016/s0009-2509(99)00098-6).
- [37] A. Saint-Jalmes, Physical chemistry in foam drainage and coarsening, *Soft Matter* 2 (10) (2006) 836–849, <https://doi.org/10.1039/b606780h>.
- [38] E. Bottaro, et al., In vitro and ex vivo evaluation of the biological performance of sclerosing foams, *Sci. Rep.* 9 (1) (2019), <https://doi.org/10.1038/s41598-019-46262-0>.
- [39] D.M. Eckmann, Polidocanol for endovenous microfoam sclerosant therapy, *Expert Opinion on Investigational Drugs* 18 (12) (2009) 1919–1927, <https://doi.org/10.1517/13543780903376163>.